AGC-2 Irradiation Creep Strain Data Analysis
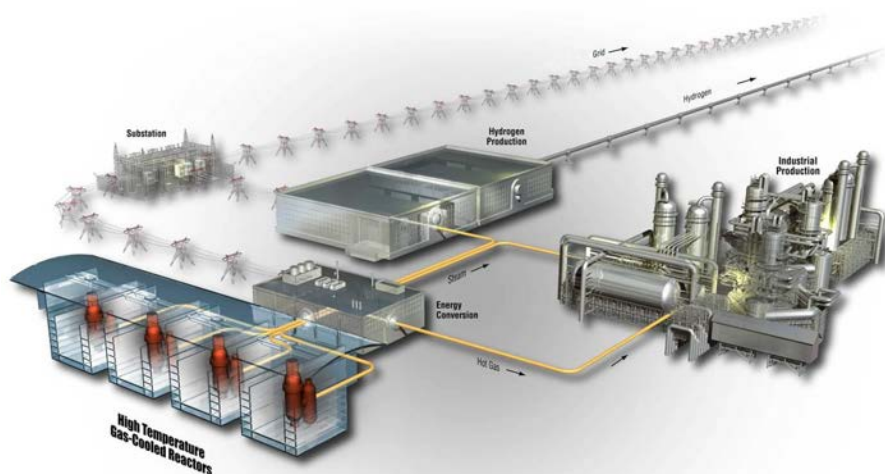
William E. Windes
David T. Rohrbaugh
W. David Swank

August 2016

INL
Idaho National
Laboratory

AGC-2 Irradiation Creep Strain Data Analysis

William E. Windes
David T. Rohrbaugh
W. David Swank

August 2016

Idaho National Laboratory
INL ART TDO Program
Idaho Falls, Idaho 83415

http://www.inl.gov
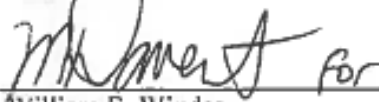
INL ART TDO Program

AGC-2 Irradiation Creep Strain Data Analysis

INL/EXT-16-39682
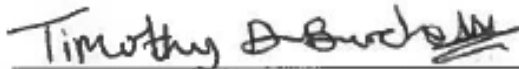**Revision 0**

August 2016

Approved by:

_____ for

William E. Windes
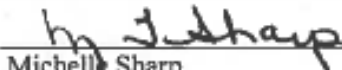Author/INL ART TDO Graphite R&D Technical Lead

8/30/16
Date

_____

Timothy D. Burchell
ORNL Graphite Technical Peer Reviewer

8 – 30 – 2016
Date

_____

Michelle Sharp
INL Quality Assurance

8/30/16
Date

_____

Hans D. Gougar
INL ART TDO Director

8/30/16
Date

SUMMARY

This report documents the analysis of the creep strain data from the Advanced Graphite Creep (AGC)-2 graphite creep specimens. This is the second of a series of six irradiation test trains planned as part of the AGC experiment to fully characterize the neutron irradiation effects and radiation creep behavior of current nuclear graphite grades. The AGC-2 capsule was irradiated in the Idaho National Laboratory Advanced Test Reactor at a nominal temperature of 600°C, beginning with irradiation Cycle 149A on April 12, 2011 and ending with Cycle 151B on May 5, 2012, with a total received dose range of 1.3–4.7 dpa.

AGC-2 was designed to provide irradiation conditions similar to AGC-1 (i.e, the same graphite grades, a nominal irradiation temperature of 600°C, and the same applied mechanical stress levels) but was irradiated for a shorter period of time to provide material property values for the graphite samples at lower dose levels than achieved in AGC-1. Material property and dimensional strain measurements were conducted on specimens from 15 nuclear graphite grades using a similar specimen assembly configuration as the first AGC capsule (AGC-1) to provide easy comparison between the two capsules. However, AGC-2 contained an increased number of specimens (i.e., 487 total specimens irradiated) and replaced specimens of the minor grade 2020 with the newer grade 2114.

Significant modifications were made to the AGC-2 irradiation capsule to improve the specimen temperature issues that were encountered with AGC-1. While the AGC-2 irradiation temperature range (399–704°C) was much narrower than AGC-1 the range is still considered less than optimal. The centrally located creep specimens (specimens under an applied mechanical stress of 13.8, 17.2, or 20.7 MPa) and control specimens (specimens with no applied stress) were irradiated over even a narrower temperature range of 541–681°C with dose levels from 2.0–4.7 dpa.

The data reported include specimen dimensions and hence the dimensional strain change upon irradiation. This allowed a comparison of these data for specimen-matched pairs yielding the dimensional and volumetric creep strain. The AGC-2 creep strain analysis methodology is similar to the AGC-1 analysis and the irradiation strain results from both capsules compare well for all grades. The derived creep coefficients have been calculated for each grade and are found to compare well to literature data, despite the larger than desired spread in specimen temperatures.

CONTENTS

FIGURES

TABLES

ix

ACRONYMS

AG	against grain
AGC	Advanced Graphite Creep
ATR	Advanced Test Reactor
HOPG	highly ordered pyrolitic graphite
HTR	high temperature reactor
INL	Idaho National Laboratory
PIE	post-irradiation examination
QA	quality assurance
WG	with grain

AGC-2 Irradiation Creep Strain Data Analysis

1.   INTRODUCTION

The Advanced Reactor Technologies Graphite Research and Development Program is conducting an extensive graphite irradiation experiment to provide data for licensing of a high temperature reactor (HTR) design. In past applications, graphite has been used effectively as a structural and moderator material in both research and commercial high temperature gas-cooled reactor designs.[1,2] Nuclear graphite H-451, used previously in the United States for nuclear reactor graphite components, is no longer available. New nuclear graphite grades have been developed and are considered suitable candidates for new HTR reactor designs. To support the design and licensing of HTR core components within a commercial reactor, a complete properties database must be developed for these current grades of graphite. Quantitative data on in-service material performance are required for the physical, mechanical, and thermal properties of each graphite grade, with a specific emphasis on data accounting for the life-limiting effects of irradiation creep on key physical properties of the HTR candidate graphite grades. Further details on the research and development activities and associated rationale required to qualify nuclear-grade graphite for use within the HTR are documented in the graphite technology research and development plan.[3]

The phenomenon of irradiation-induced creep within graphite has been shown to be critical to the total useful lifetime of graphite components. Irradiation-induced creep occurs under the simultaneous application of neutron irradiation and applied stresses within the graphite components. Significant internal stresses within the graphite components can result from a second phenomenon due to dose and temperature gradients—irradiation-induced dimensional change—where the graphite physically changes (i.e., first shrinking and then expanding with increasing neutron dose). This disparity in material volume change can induce significant internal stresses within graphite components. Irradiation-induced creep relaxes these large internal stresses, thus reducing the risk of crack formation and component failure. Higher levels of irradiation creep will relieve more internal stress providing the components longer useful lifetimes within the core. Determining the irradiation creep rates of nuclear graphite grades is critical for determining the useful lifetime of graphite components and is a major component of the Advanced Graphite Creep (AGC) experiment.

The AGC experiment is currently underway to determine the in-service behavior of these new graphite grades for HTR. This test series will examine the properties and behaviors of nuclear-grade graphite over a large spectrum of temperatures, irradiation fluence, and applied stress levels that are expected to induce irradiation creep strains within an HTR graphite component. Irradiation data are provided through the AGC test series, which comprises six planned capsules irradiated in the Advanced Test Reactor (ATR) in a large flux trap at Idaho National Laboratory (INL). The AGC irradiation conditions are similar to the anticipated environment within a high temperature core design. Each irradiation capsule is composed of more than 400 graphite specimens that are characterized before and after irradiation to determine the irradiation-induced changes in material properties and the rate of life-limiting irradiation creep for each graphite grade.

This report provides an AGC post-irradiation examination (PIE) analysis of the irradiation-induced creep strain within the second AGC capsule (AGC-2). The AGC-2 calculated creep coefficients were compared with AGC-1 values along with historical data from literature to ascertain any significant trends in the data. In this way, the consistency and soundness of the data are initially tested and validated from previous creep analyses.

1

The data and information produced in this document and the referenced documents within were generated under the approved quality assurance (QA) programs for the respective organizations, including INL and Oak Ridge National Laboratory in compliance with the appropriate NQA-1 requirements. It is anticipated that all data will be robust enough to stand up to a review by the Nuclear Regulatory Commission as support for a graphite reactor design selection.

2. ADVANCED GRAPHITE CREEP EXPERIMENT

The AGC test series is designed to establish the data necessary to determine the safe operating envelope of graphite core components for an HTR by measuring the irradiated material property changes and the behavior of several new nuclear graphite grades over a large range of temperatures, neutron fluence, and mechanical compressive loads. The experiment consists of three interrelated stages: pre-irradiation characterization of the graphite specimens, the irradiation test series (designated as six separate irradiation test train capsules), and PIE and analysis of the graphite specimens after irradiation. Separate reports for each distinct stage are prepared after each individual activity is completed.

The pre-irradiation examination report details the total number of graphite grades and individual specimens, the specimen loading configuration designed to expose all specimens to the entire range of irradiation conditions, and the pre-irradiation material property testing data and results. The as-run irradiation report details the irradiation history of each capsule while in the reactor, noting any changes from the technical and functional specifications for each specific test series capsule and identifying the possible improvements to the next test series capsule design. The disassembly report details specimen recovery from the irradiation capsule, noting any damage to the specimens and providing an inventory of recovered specimens for PIE testing. The PIE data report details the changes in specimen dimensional measurements as well as irradiated material properties upon exposure to neutron irradiation. Finally, the PIE analysis report analyzes the irradiation results reported within the data package reports, utilizing the irradiation conditions recorded within the as-run irradiation report. The PIE analysis report(s) contain the determinations of irradiation-induced creep rates for the major grades of graphite and assessments of any changes to the material properties in all graphite grades. The PIE analysis report(s) interpret the irradiation behavior of graphite to assist in determining a credible, safe operating envelope for graphite core components in an HTR design and licensing application.

This report is an AGC PIE analysis report on irradiation-induced creep strain within the second AGC capsule (AGC-2). Data from the "AGC-2 Specimen Post-Irradiation Data Package Report"[4] was used to analyze the dimensional strain data in order to calculate the corresponding creep strain and creep coefficients for each graphite grade. An analysis of the irradiation material property changes (electrical resistivity, thermal diffusivity, coefficient of thermal expansion, stiffness, and strength) will be provided within a future PIE analysis report.

2.1 Design Parameters of AGC Experiment

The AGC test series is designed to measure changes in key thermal, physical, and mechanical material properties over the anticipated range of HTR operating conditions. By comparing the material properties of each specimen before and after irradiation, the experiment generates quantitative material property change data and irradiation creep data that will be used to predict the in-service behavior and operating performance of the current nuclear graphite grades for HTR designs. Specific emphasis is placed on data that pertain to the life-limiting effects of irradiation creep on graphite components and the effects creep may have on key irradiated material properties of several candidate graphite grades for use in an HTR design.

The critical component of the experiment is the irradiation test series, which irradiates the graphite specimens after pre-irradiation examination characterization has been completed. The AGC test series is

2

composed of six planned irradiation test trains that are irradiated in ATR in a large flux trap, as described in the "Graphite Technology Development Plan."[3] The test series exposes test specimens of select nuclear graphite grades to temperatures and the initial range of irradiation dose that are expected within an HTR design. Specifically, graphite specimens will be exposed to a fast neutron dose ranging from 1 to 7 dpa and temperatures of 600, 800, and 1,100°C, as shown in Figure 1. The first and second AGC capsules, AGC-1 and AGC-2, were designed to be irradiated within the ATR's south flux trap.[5] All other AGC capsules will be irradiated within ATR's east flux trap. Generally, irradiations within the south flux trap require approximately 175 effective full-power days to provide a nominal fast neutron dose range (in graphite) of approximately 0.5–3.5 dpa. For capsules requiring a large dose range of approximately 3.5–7.0 dpa, the irradiation capsule (containing the graphite specimens) is irradiated for twice as long inside the ATR, approximately 350 effective full-power days.
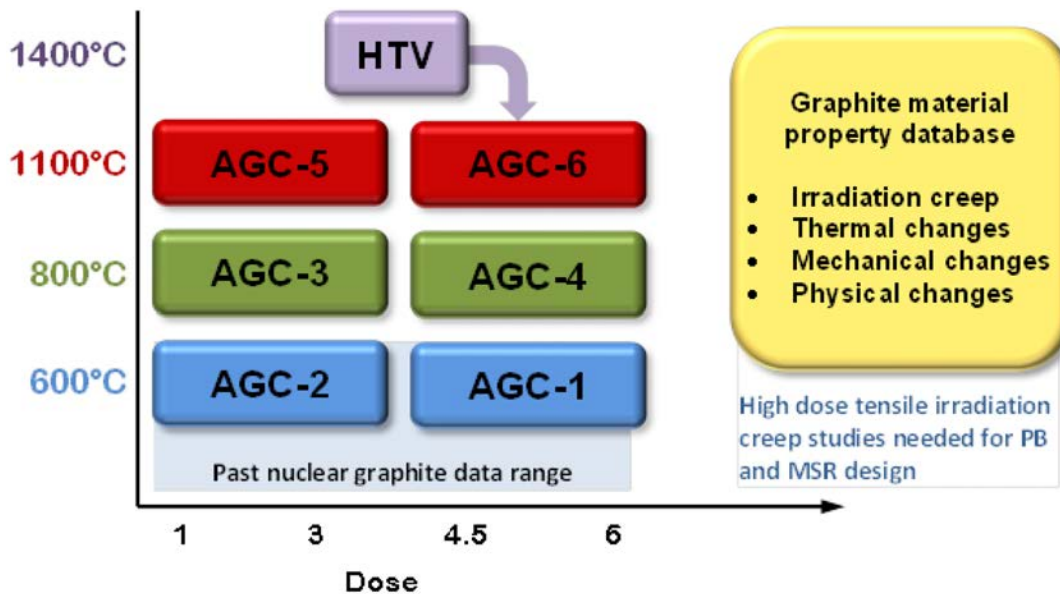
Figure 1. Irradiation dose and temperature parameters for the AGC experiment (HTV = high temperature vessel, MSR = Molten Salt Reactor, PB = Pebble Bed).

In addition to determining the irradiation-induced changes to the material properties of selected nuclear graphite grades, the AGC experiment dedicates a significant amount of scope to determining rates of irradiation-induced creep for different nuclear graphite grades. The traditional method for measuring irradiation-induced creep is to apply a significant mechanical load (inducing a mechanical stress within the graphite) to half the specimens during irradiation while leaving the remaining half of the specimens unloaded (unstressed). Mechanically loaded (stressed) specimens are traditionally designated as the creep specimens, and the unloaded (unstressed) specimens are designated as the control specimens. The resulting difference in dimensional change between the loaded and unloaded specimens (assuming that temperature and dose levels are the same) provides the amount of irradiation-induced strain for each "matched pair" of graphite specimens. From this strain level, a creep rate for each graphite grade can be calculated as a function of dose if both specimens were irradiated at the same constant temperature and dose level. Thus, each capsule is designed to be irradiated at a constant temperature, allowing only the dose and applied mechanical load to vary within the test train of each test-series capsule. With all graphite specimens at a constant temperature, only the applied stress level and dose will affect the calculated creep rate of each graphite grade within a test series capsule.

The AGC experiment is designed to measure the constant creep strain behavior (secondary creep) of the various grades. The experiment assumes that the induced creep strain for all specimens is within the secondary creep regime and therefore behaves linearly with respect to received neutron dose.[3] This assumption is valid provided the specimens do not go beyond their turnaround dose where creep strain can no longer be expected to be linear with irradiation dose (the onset of tertiary creep). Once the specimens begin to reach turnaround, the creep strain response becomes nonlinear with received dose. To ensure specimens remain within the constant linear creep strain regime within AGC-5 and AGC-6 (the highest temperature and dose) test trains, a high temperature irradiation vessel will be used to measure the dimensional changes of the graphite grades at a high temperature (1,400°C) and moderate dose (4.5 dpa). Results from this high temperature dimensional change study will be utilized in the AGC-5 and AGC-6 designs, which constitute the upper bounds of the AGC experiment (Figure 1). In addition, if any graphite grade achieves turnaround within the high temperature irradiation vessel, the graphite grade will be considered to be outside the upper bounds of the AGC experiment and will be eliminated from the AGC-6 test train.

While the effects from applied mechanical stresses and neutron dose can be determined within each irradiation capsule, the temperature dependency of any irradiation-induced material property changes within the graphite grades is achieved by comparing the measured values of the specimens between irradiation capsules. Because each test train is irradiated at a constant temperature (600, 800 or 1,100°C), the temperature-induced/enhanced material property changes must be determined by comparing specimens in different capsules exposed to similar doses and applied mechanical load levels. All AGC capsules are designed to have the same specimen stacking patterns. Thus, if specimens of identical graphite grades are located in similar positions within each capsule, a similar dose and load level will be imposed on a consistent grade of graphite. Maintaining consistent specimen positions for each grade within the six different capsules will allow the determination of temperature-induced changes for irradiation creep and material properties across the AGC experiment.

2.2   AGC Graphite Grades and Specimen Dimensions

The AGC experiment is designed to ascertain the irradiation behavior of currently available nuclear graphite grades within the anticipated operating parameters of an HTR design. By exposing a variety of nuclear graphite grades representing the range of fabrication parameters (grain size, fabrication processes, and raw source material) to the expected operating conditions for an HTR design (600–1,100°C and 0.5– 7 dpa dose), a comprehensive understanding of the irradiation response and behavior of graphite components in general can be achieved. This will limit the need for additional research in the future if the current graphite grades are altered (i.e., new raw material sources are used) or new grades are utilized in future reactors.

The AGC experiment utilizes a variety of current graphite grades to envelope the major fabrication parameters believed to be responsible for the irradiation behavior of nuclear graphite.[1] This range of fabrication parameters is represented by AGC major grades, which were deemed to be production-ready grades that could be used in current or future HTR designs. Major graphite grades are one type of sample within the AGC irradiation capsule. In addition, four other sample types are designated within the AGC experiment. The five AGC sample types are categorized as follows:[6]

1. Major Grades (Irradiation Creep and Control Specimens)

    These graphite grades are current reactor candidates for the core structures of an HTR design as well as historical (reference) grades. Due to their fabrication maturity and consistency, HTR core components are most likely to be formed from these major grades and are thus expected to receive reasonably large neutron doses in their lifetime. Only major grade specimens were used to determine the critical irradiation-induced creep strain rate.

4

2. Minor Grades (Piggyback Specimens)

These grades are HTR-relevant grades that are not yet production ready or are most likely to be used in low neutron dose regions of the core (e.g., the permanent structure of the prismatic block HTR design).

3. Alternate Grades (Piggyback Specimens)

These are grades that current HTR vendors have identified as being of interest as alternate graphite grades for certain components within the reactor.

4. Experimental Grades (Piggyback Specimens)

Experimental graphite grades are included in AGC to assess the viability of new graphite grades whose manufacturing processes and raw materials are such that they may offer superior irradiation stability. Additionally, other carbonaceous materials such as fuel compact matrix materials, carbon-carbon composites, silicon-carbide composites, or other experimental materials that could offer superior performance within the extreme environment of an HTR core are included.

5. Single Crystal Graphite (Piggyback Specimens)

Samples of highly ordered pyrolytic graphite (HOPG) are included in AGC to assess the fundamental irradiation response of single crystal graphite. These specimens offer specific dimensional change behavior of graphite, which is particularly significant to the behavior of polycrystalline (polygranular) graphite grades.

To provide all necessary material property tests in the AGC experiments, each test series capsule contains two primary specimens: (1) "creep" specimens, providing irradiation creep-rate behavior as well as mechanical property behavior and (2) "piggyback" specimens, providing thermal material property behavior for the graphite. Creep specimens are fabricated only from major grade graphite types.[2,7,8] Piggyback specimens are fabricated from major, minor, and experimental grade graphite. The piggyback specimens are not mechanically loaded and are subjected only to neutron irradiation at high operating temperatures to assess the effects of a reactor environment on the specific graphite grade.

All specimens are 12.7 mm (0.5 in.) in diameter, with the larger creep specimens being 25.4 mm (1.0 in.) long and the button-sized piggyback specimens being 6 mm (0.25 in.) long. Small graphite containers that are 12.7 mm in diameter by 6 mm long contain the thin wafer HOPG specimens. The large creep specimens provide accurate dimensional change, elastic modulus, thermal expansion, electrical resistivity, and mechanical strength measurements. However, the longer creep specimens make them unsuitable for thermal diffusivity measurements. The small piggyback specimens permitted only dimensional measurements, density testing, and thermal-diffusivity testing to be performed. Together, both types of specimens provide the changes in material properties for stressed (creep) and unstressed (control) graphite grades.[8]

2.3   General AGC Test Train Design

All AGC test trains and irradiation capsules have the same general physical configuration to provide consistent dose and applied mechanical stresses on specimens of similar graphite grades. While there are key machining and structural differences between capsules to change the irradiation temperature for the different capsules, the majority of the AGC design is identical for all capsules. A schematic of the AGC-2 test train and location of graphite specimens within the test train is shown in Figure 2.[9]
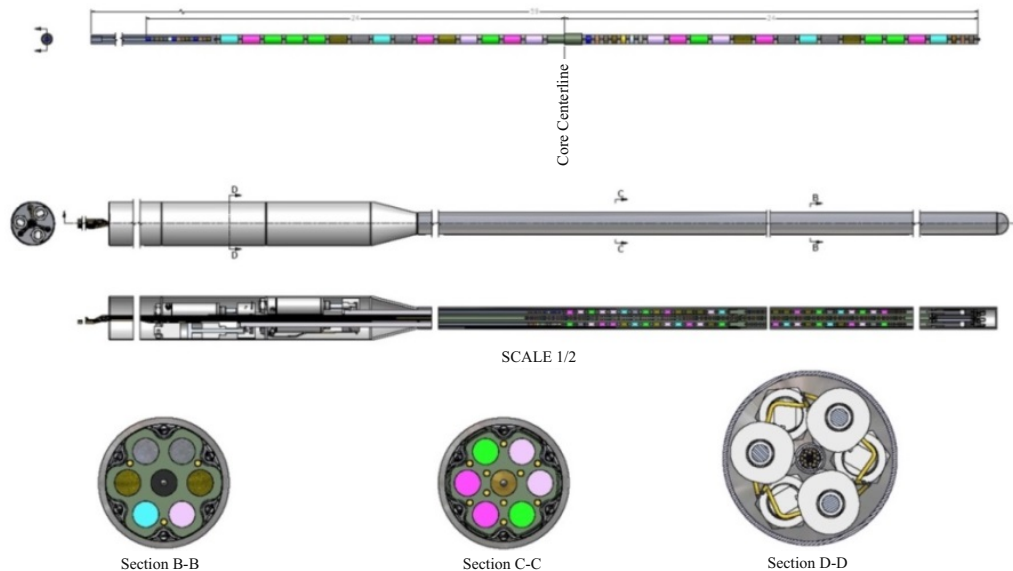
Figure 2. The AGC-2 creep capsule.

All irradiation capsules have six channels located in the outer perimeter of the graphite specimen holder body and a center channel. All channels are 12.9 mm (0.51 in.) in diameter and are designed to hold all types of AGC specimens. The upper (top) half the outer channels has mechanical loads applied to the specimens. However, the lower (bottom) half for these channels has no mechanical load applied to the specimens in these locations. Due to the neutron flux profile in ATR, matched pairs with similar neutron fluence and temperatures are achieved by pre-ordering the specimen axial locations. Specimens in the upper half of the channels were stressed by the applied mechanical load while their matched pair received a similar dose in an unstressed state. Three stress levels—13.8 MPa, 17.2 MPa, and 20.7 MPa (2.0 ksi, 2.5 ksi, and 3.0 ksi) nominal—are applied in all AGC capsules to provide a known stress on the graphite specimens during irradiation. These induced stress levels are high enough to produce irradiation-induced creep strain with the graphite specimens.

Temperature values within all AGC capsules are calculated based on thermocouple readings at select positions within the capsule. Specimen temperature is calculated with a finite element model that has been calibrated to predict the known thermocouple readings in the capsule. Dose levels are calculated using Monte Carlo N-Particle Transport Code models and operating conditions in the ATR core and are corroborated from flux wire data.

2.4   Establishing Specimen Dose and Applied Load

To achieve the desired irradiation dose levels and applied mechanical loads to the specific specimens, an exact specimen loading order is critical. Because irradiation creep is usually determined by the difference in dimensional change occurring within specimens that have an applied load and those that do not, these "matched pair" specimens are assumed to have the same irradiation dose and irradiation temperature values. The AGC test train designs utilize the symmetric flux profile generated within the ATR to achieve these similar irradiation conditions for "matched pairs."

Specimens within the upper half of the capsule have a mechanical load applied to them via a pneumatic ram system. Specimens within the lower half remain unloaded and thus have no applied stress. The ATR specimens in the upper half of the capsule are located in positions that receive a dose level similar to their "matched pair" specimens in the lower half of the capsule. A careful specimen loading

order within the irradiation capsule is required to ensure similar dose levels for each "matched pair."[10,11] Other considerations include the size of each creep specimen, the need for periodically placed spacers containing flux wires, and the space requirements in the top of the stacks for the pneumatic push rods. The core flux mid-plane, in relation to the capsule arrangement, was established so that the reactor neutron flux field could be correlated to the physical elevations and positions in the capsule to yield accurate "match pair" irradiation dose levels, Figure 3.[12]
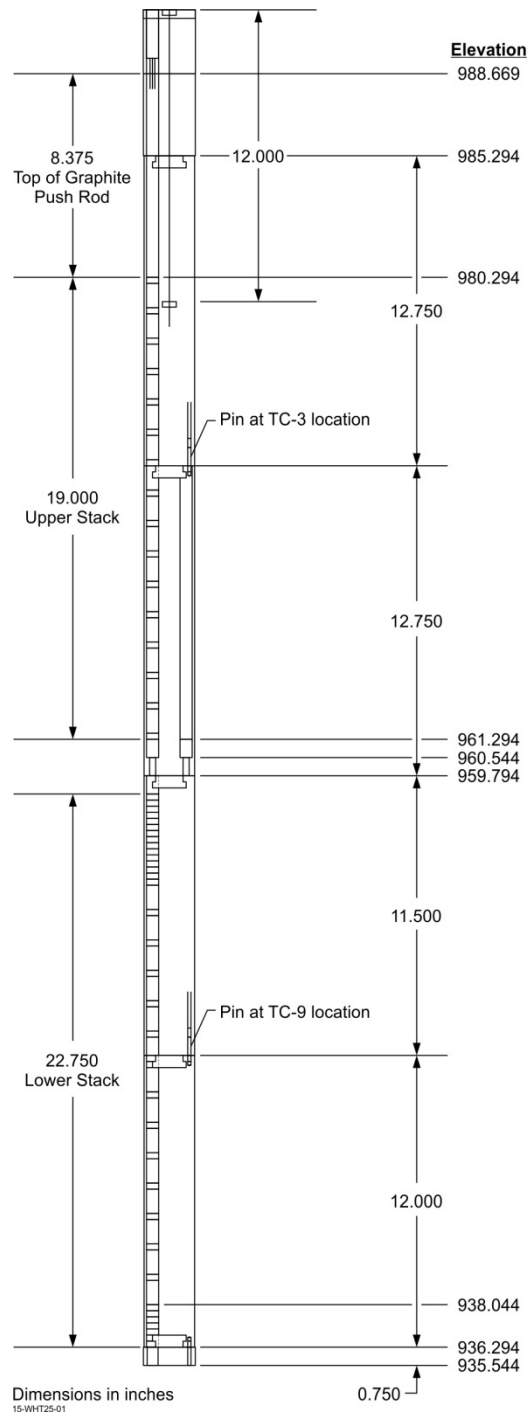
Figure 3. Elevation sketch of the AGC capsule.

Irradiation dose values, as a function of distance from the reactor core centerline, are calculated from the total calculated fluence using standard conversion factors for carbon in a fast neutron irradiation field (E >0.1 MeV).[13] A neutron flux gradient across the capsule thickness requires the capsule to be rotated 180 degrees at the irradiation midpoint. This rotation results in a uniform neutron-fluence profile for all stacks, regardless of their position within the capsule.

As described in previous reports,[6] the ATR neutron flux profile is not completely symmetrical along the vertical axis. Thus, to produce matched-pair specimens that have similar dose profiles both above and below the core mid-plane, an offset position from the mid-plane is required. An offset distance of 31.75 mm (1.25 in.) from the core mid-plane for the bottom creep specimens produces the closest dose matches between specimens. While it was impossible to exactly match the dose levels for both the upper and lower specimens, the dose levels for each specimen pair were fairly close, ranging from 0–2%.[14]

2.5   Physical Positions of Creep Specimens in the Stacks

Once the specimen-position offset is established for the bottom half of the specimens, the number of total creep specimens for each grade of graphite is determined. It should be noted that the specimen stacking order for subsequent AGC irradiation capsules was changed from that initially established for the AGC-1 test train. In the initial AGC capsule design, AGC-1 utilized 6.35 mm (0.25 in.) long NBG-25 graphite spacers between all creep specimens to separate them from each other. It was determined that this was not necessary, and most of the 6.35 mm (0.25 in.) long NBG-25 graphite spacers were eliminated. The decision to eliminate the spacers increased the total number of creep specimens in the AGC capsules to 216 total specimens (or 36 matched pairs in each outer perimeter channel). This allowed more specimens per graphite grade to be irradiated within the AGC-2 capsule.

As mentioned above, the six outer stacks in the capsule allow the specimens in two of the channel stacks to be loaded at 13.8 MPa, while the other two pairs of channels are loaded at 17.2 and 20.7 MPa, respectively. Because two stacks are at similar applied stress levels, the specimen loading order can be shifted between the two stacks, allowing the same grade of graphite to be mechanically loaded over a broader neutron dose range, as illustrated in Figure 4. Assuming that both stacks will have the same applied stress level, receive similar dose levels per position, and have a constant temperature allows this shifting of the specimens and, consequently, a more uniform, smoother dose profile for each graphite grade.

A final consideration when establishing the specimen loading positions is the grain orientation of the specimens. All AGC capsules attempt to account for the grain orientation relative to irradiation behavior. For extruded graphite grades, the against-grain (AG) and with-grain (WG) directions are obviously perpendicular and parallel to the extrusion direction, respectively. Isomolded grades have little to no grain direction and there is no consideration for their orientation. However, in the case of the vibration-molded graphites (i.e., NBG-17 and -18), there are actually two WG directions and one AG direction as a consequence of the fabrication process. The total number of WG and AG specimens is dependent on the particular AGC capsule pair (i.e., AGC-1 and AGC-2 have the same number of specimens with similar orientation).

Once these considerations are accounted for, the dose-level profiles are determined for each graphite grade within each channel stack. It should be noted that due to the elimination of the majority of the NBG-25 spacers from the AGC-1 design, the dose-level profiles for each graphite grade have been altered for the succeeding AGC capsules. [15,16,17] However, the changes are modest, allowing nearly direct comparison between AGC-1 and the subsequent AGC capsules.
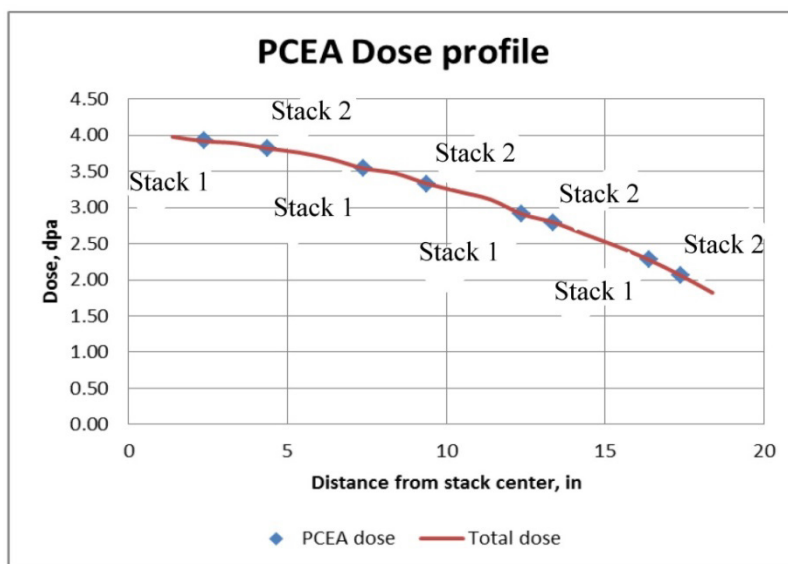
Figure 4. A typical dose profile for creep graphite specimens utilizing similar applied stress levels in matched stacks.

3. AGC-2 TEST TRAIN CAPSULE

The AGC-2 capsule was irradiated in the ATR beginning with Cycle 149A on April 12, 2011 and ending with ATR Cycle 151B on May 5, 2012.[18] In general, the average estimated irradiation temperature for all samples in the AGC-2 test train was 600°C with a standard deviation of 64°C and a total range of 392–707°C. The average radiation dose of all specimens was 3.41 dpa with a standard deviation of 1.03 dpa and a total range of ~1.26–4.66 dpa. This includes the piggyback specimens in the extreme top and bottom positions of the irradiation capsule. While the temperature range was much better than the prototype AGC-1 irradiation capsule, the AGC-2 irradiation temperature range exceeded the design $(600 \pm 50°C)$.[19] Irradiation temperature, applied stress, and total received dose levels for the AGC-2 creep and control specimens have much narrower ranges due to their centralized position within the irradiation capsule. Specific creep and control specimen irradiation ranges are reported later in this analysis report. All AGC-2 design documents and drawings pertinent to the AGC-2 graphite specimens have been reported in the previous AGC-2 graphite pre-irradiation data package, INL/EXT-10-19588.[20]

The AGC-2 irradiation capsule is the companion capsule for AGC-1. The original AGC-2 capsule design was intended to be a mirror of AGC-1 but would be irradiated within ATR for twice as long to achieve the higher dose levels. However, due to the large and unintended temperature variation across the AGC-1 capsule, it was decided that AGC-1 would be exposed to the higher neutron dose (i.e., nominal 3.5–7 dpa) to provide additional high dose data. Consequently, the AGC-2 design was modified to provide the lower dose data across a range of 1–5 dpa (i.e., the capsules were reversed with AGC-1 being the higher dose capsule and AGC-2 being the lower dose capsule).[19] The ATR irradiation cycles were chosen to achieve this new dose range.

While some significant modifications were made to the AGC-2 irradiation specimens and layout (e.g., the elimination of the majority of NBG-25 spacers to provide more space for creep specimens), the overall design of AGC-2 was kept as close to AGC-1 as possible. All minor and experimental graphite grades were retained, and only one alternate graphite grade was replaced with a new nuclear grade. This allows results from both capsules to be compared and combined into a larger data population.

9

3.1 Design Parameters of AGC-2 Test Train

It was decided that AGC-2 and subsequent capsules did not require the addition of silicon carbide temperature monitors to provide independent temperature verification during capsule irradiation.[21] Consequently, the central hole in each of the central piggyback specimens was not machined to accommodate the silicon carbide temperature monitors. By eliminating these monitors, the independent temperature monitoring capability for the AGC-2 capsule was excluded, but it was determined that being able to measure the changes to the thermal diffusivity at high temperatures was more important. Central holes in all subsequent AGC piggyback specimens for the remaining AGC irradiation capsules were eliminated.[8]

As discussed previously, a majority of the 6.35 mm (0.25 in.) long NBG-25 graphite spacers between all AGC-1 creep specimens was eliminated. Four spacers were left in each channel (two in the upper section of the channel and two in the lower section) to allow flux wires to be placed within them. Eliminating most of the spacers allowed 12 additional creep specimens to be tested within the AGC-2 capsule. The total number of creep specimens in the AGC-2 capsule was increased to 216 total specimens (or 36 matched pairs in each outer perimeter channel).[20] This stacking configuration with minimal spacers will be used with subsequent AGC irradiation capsules (i.e., AGC-3, AGC-4, etc.).

3.2 AGC-2 Graphite Grades and Changes to Dimensions

One of the graphite grades in AGC-2 was changed by request of the graphite vendor (Mersen, USA). Piggyback specimens of graphite grade 2114 were directly substituted for graphite grade 2020 and irradiated within the AGC-2 central stack (axial spine of capsule). All other graphite grades irradiated within AGC-2 were similar to the graphite grades in AGC-1. However, the sample numbers for two major grades, H-451 and IG-430, were reduced to allow for more creep test specimens in the remaining major grade graphite.

The major grades of the nuclear graphite to be tested in AGC-2 are similar to AGC-1 major grades and include NBG-17, NBG-18, PCEA, IG-110, H-451, and IG-430. Minor, alternate, and experimental grades of graphite are presented below:

1. Major graphite grades: NBG-17, NBG-18, PCEA, IG-110, H-451, and IG-430

2. Minor graphite grades: NBG-25, NBG-10, HLM, PGX

3. Alternate grades: PPEA, PCIB, and 2114 (replaced grade 2020)

4. Experimental grades: BAN and A3-3/A3-27 fuel compact matrix material

5. Single crystal graphite: HOPG.

A more complete description of all of the graphite samples included in capsule AGC-2 is given in Table 1.[20] Code letters were given to each graphite grade in replace of their name designations to shorten the specimen identification number for each specimen. This allowed the specimen to have a short ID number which was necessary for the laser engraving of each specimen. For grades NBG-17, NBG-18, and PCEA (codes A, B, and D) both WG and AG specimen orientations are included in the capsule.

Table 1. Major, minor, alternate, and experimental graphite grades within the AGC-2 capsule.

Graphite Grade	Forming Method	Intended Purpose	AGC Code Letter
NBG-17	Vibrational molded	AREVA Next Generation Nuclear Plant design	A
NBG-18	Vibrational molded	Pebble Bed modular reactor (not currently being pursued)	B
H-451	Extruded	Historical grade (Reference grade)	C
PCEA	Extruded	AREVA Next Generation Nuclear Plant design	D
IG-110	Isostatically pressed	HTR – Pebble-Bed module (China)	E
IG-430	Isostatically pressed	Candidate graphite	F
HOPG	Vapor deposited	Fundamental studies	G
A3 matrix	Hot pressed	Fuel matrix material	H
HLM	Molded	Low dose core component	J
PGX	Extruded	Low dose core component	K
PPEA	Extruded	Alternate candidate	L
NBG-25	Isostatically pressed	Low dose core component	M
PCIB	Isostatically pressed	Alternate candidate	P
BAN	Isostatically pressed and extruded	Experimental graphite	R
NBG-10	Isostatically pressed	Low dose core component	S
2114	Isostatically pressed	Candidate graphite	T

3.3 AGC-2 Specimen Stack Positions

The final loading configuration for the outer channel/stacks was determined for each graphite grade to optimize the number of specimens for each grade, create a smooth irradiation profile for the creep and piggyback specimens, and ensure the proper position of creep specimens to create the matched pairs.

A further decision was made to increase the creep specimen number population for the newer graphite grades, because little-to-no irradiation data are available on these grades. Specifically, more specimens of graphite grades NBG-18 and PCEA were chosen to be irradiated instead of the IG-110, IG-430, and NBG-17 graphite grades[20]. NBG-18 and PCEA were determined to have 16 specimens per applied stress level for a total of 48 specimens within AGC-2. Graphite grades IG-110 and IG-430 were represented by only 12 specimens per applied stress level, for a total of 36 specimens within AGC-2. Table 2 lists the total number of specimens irradiated per major graphite grade.

Table 2. Total number of irradiated-creep specimens in the AGC-2 test series capsule.

Graphite Grade	Number of Creep Specimens
PCEA	48
NBG-18	48
IG-110	36
IG-430	36
NBG-17	24
H-451	24
Total Creep	216

In AGC-2, approximately 75% of extruded specimens (H-451 and PCEA) were oriented in the WG direction and 25% of the specimens were AG. As discussed previously, isomolded grades (IG-110 and IG-430) have little to no grain direction and there is no consideration of specimen orientation for these grades. However, in the case of the vibration-molded graphite grades (i.e., NBG-17 and -18), which possess two WG directions and one AG direction[2] it was logical to split the WG and AG specimens evenly (i.e., 50/50 ratio) rather than following the 75/25 ratio established for the extruded specimens.

The orientation of the specimen is designated by the second digit in the sample identification number. Specimen identification numbers possessing a "W" in the second digit are specimens in the WG orientation (e.g., CW101). Specimen identification numbers possessing an "A" in the second digit are specimens machined from an AG orientation (e.g., DA402). As discussed previously, vibrationally molded grades are designated with an "L" or "P" for the two WG orientations (e.g., BP402 for an NBG-18 grade specimen).

The final loading configuration for AGC-2, including creep specimen matched-pair positions (above and below the capsule mid-plane), piggyback order, lower stack offset, and flux wire spacers, was mapped for each graphite specimen as it was loaded into the AGC-2 irradiation capsule during assembly (Table 3 through Table 6).[20,22]

Table 3. AGC-2 loading order for Stacks 1 and 2 (Position taken in middle of specimen or COM - Center of Mass).

S-1, Compressed

Work Order 137268 Loading Order	Work Order 137268 ID Number	Graphite Type	Initial Specimen COM Elevation (in)
23	CW101	H451	19.500
22	1A	Flux Monitor	18.875
21	DW101	PCEA	18.250
20	BW101	NBG-18	17.250
19	EW0102	IG-110	16.250
18	FW0101	IG-430	15.250
17	DW102	PCEA	14.250
16	AY	Flux Monitor	13.625
15	BW102	NBG-18	13.000
14	FW0102	IG-430	12.000
13	EW0104	IG-110	11.000
12	DW1001	PCEA	10.000
11	BW103	NBG-18	9.000
10	FW0103	IG-430	8.000
9	1H	Flux Monitor	7.375
8	CW102	H451	6.750
7	EW0201	IG-110	5.750
6	DW1002	PCEA	4.750
5	BW1001	NBG-18	3.750
4	FW0104	IG-430	2.750
3	8H	Flux Monitor	2.125
2	AW101	NBG-17	1.500

S-2, Compressed

Work Order 137268 Loading Order	Work Order 137268 ID Number	Graphite Type	Initial Specimen COM Elevation (in)
23	EW0301	IG-110	19.500
22	AW1707	NBG-17	18.875
21	FW0301	IG-430	18.250
20	DA402	PCEA	17.250
19	BP402	NBG-18	16.250
18	AW103	NBG-17	15.250
17	EW0302	IG-110	14.250
16	2B	Flux Monitor	13.625
15	DW1103	PCEA	13.000
14	BW1103	NBG-18	12.000
13	CW1003	H451	11.000
12	AW1001	NBG-17	10.000
11	EW0303	IG-110	9.000
10	DA403	PCEA	8.000
9	AW1708	NBG-17	7.375
8	BP403	NBG-18	6.750
7	FW0302	IG430	5.750
6	AP402	NBG-17	4.750
5	CW1101	H451	3.750
4	DW1104	PCEA	2.750
3	37	Flux Monitor	2.125
2	BW1201	NBG-18	1.500

S-1, Uncompressed

Work Order 137268 Loading Order	Work Order 137268 ID Number	Graphite Type	Initial Specimen COM Elevation (in)
36	AW102	NBG-17	-1.750
35	AO	Flux Monitor	-2.375
34	FW0201	IG-430	-3.000
33	BW1002	NBG-18	-4.000
32	DW1003	PCEA	-5.000
31	EW0202	IG-110	-6.000
30	CW103	H451	-7.000
29	AL1402	NBG-17	-7.625
28	FW0202	IG-430	-8.250
27	BW1003	NBG-18	-9.250
26	DW1004	PCEA	-10.250
25	EW0203	IG-110	-11.250
24	FW0203	IG-430	-12.250
23	BW1101	NBG-18	-13.250
22	8U	Flux Monitor	-13.875
21	DW1101	PCEA	-14.500
20	FW0204	IG-430	-15.500
19	EW0204	IG-110	-16.500
18	BW1102	NBG-18	-17.500
17	DW1102	PCEA	-18.500
16	AE	Flux Monitor	-19.125
15	CW1002	H451	-19.750
14	BP7 06	NBG-18	-20.375
13	L2 08	PPEA	-20.625
12	K2 09	PGX	-20.875
11	P2-08	PCIB	-21.125
10	DW18 03	PCEA	-21.375
9	M2 07	NBG-25	-21.625
8	S2 07	NBG-10	-21.875
7	FW15 01	IG-430	-22.125
6	EW14 01	IG-110	-22.375
5	J2 06	HLM	-22.625
4	RW2 09	BAN	-22.875
3	H562	Compact Matrix	-23.125
2	TP 18	2114	-23.375

S-2, Uncompressed

Work Order 137268 Loading Order	Work Order 137268 ID Number	Graphite Type	Initial Specimen COM Elevation (in)
36	BW1202	NBG-18	-1.750
35	AW1709	NBG-17	-2.375
34	DW1201	PCEA	-3.000
33	CW1102	H451	-4.000
32	AP403	NBG-17	-5.000
31	FW0303	IG-430	-6.000
30	BP501	NBG-18	-7.000
29	EW1509	IG-110	-7.625
28	DA501	PCEA	-8.250
27	EW0304	IG-110	-9.250
26	AW1002	NBG-17	-10.250
25	CW1103	H451	-11.250
24	BW1203	NBG-18	-12.250
23	DW1202	PCEA	-13.250
22	7D	Flux Monitor	-13.875
21	EW0401	IG-110	-14.500
20	AW1003	NBG-17	-15.500
19	BP502	NBG-18	-16.500
18	DA502	PCEA	-17.500
17	FW0304	IG-430	-18.500
16	EW1510	IG-110	-19.125
15	EW0402	IG-110	-19.750
14	J2 07	HLM	-20.375
13	RW2 10	BAN	-20.625
12	H571	Compact Matrix	-20.875
11	TP19	2114	-21.125
10	BP7 07	NBG-18	-21.375
9	L2 09	PPEA	-21.625
8	K2 10	PGX	-21.875
7	P2-09	PCIB	-22.125
6	DW18 04	PCEA	-22.375
5	M2-08	NBG-25	-22.625
4	S2 08	NBG-10	-22.875
3	FW15 02	IG-430	-23.125
2	EW14 02	IG-110	-23.375

Table 4. AGC-2 loading order for Stacks 3 and 4 (Position taken in middle of specimen or COM - Center of Mass).

S-3, Compressed

Work Order 137268 Loading Order	Work Order 137268 ID Number	Graphite Type	Initial Specimen COM Elevation (in)
23	CW1202	H451	19.500
22	TP 27	2114	18.875
21	DW1203	PCEA	18.250
20	BW1301	NBG-18	17.250
19	EW0403	IG-110	16.250
18	FW0401	IG-430	15.250
17	DW1204	PCEA	14.250
16	2U	Flux Monitor	13.625
15	BW1302	NBG-18	13.000
14	FW0402	IG-430	12.000
13	EW0404	IG-110	11.000
12	DW1301	PCEA	10.000
11	BW1303	NBG-18	9.000
10	FW0404	IG-430	8.000
9	TP 12	2114	7.375
8	CW1203	H451	6.750
7	EW0501	IG-110	5.750
6	DW1302	PCEA	4.750
5	BW1401	NBG-18	3.750
4	FW0501	IG-430	2.750
3	8Y	Flux Monitor	2.125
2	AW1101	NBG-17	1.500

S-4, Compressed

Work Order 137268 Loading Order	Work Order 137268 ID Number	Graphite Type	Initial Specimen COM Elevation (in)
23	EW0601	IG-110	19.500
22	AX	Flux Monitor	18.875
21	FW0602	IG-430	18.250
20	DA503	PCEA	17.250
19	BP503	NBG-18	16.250
18	AW1103	NBG-17	15.250
17	EW0602	IG-110	14.250
16	18	Flux Monitor	13.625
15	DW1403	PCEA	13.000
14	BW1503	NBG-18	12.000
13	CW1303	H451	11.000
12	AW1201	NBG-17	10.000
11	EW0603	IG-110	9.000
10	DA601	PCEA	8.000
9	AR	Flux Monitor	7.375
8	BP601	NBG-18	6.750
7	FW0603	IG-430	5.750
6	AP501	NBG-17	4.750
5	CW201	H451	3.750
4	DW1404	PCEA	2.750
3	3F	Flux Monitor	2.125
2	BW1601	NBG-18	1.500

S-3, Uncompressed

Work Order 137268 Loading Order	Work Order 137268 ID Number	Graphite Type	Initial Specimen COM Elevation (in)
36	AW1102	NBG-17	-1.750
35	TP24	2114	-2.375
34	FW0502	IG-430	-3.000
33	BW1402	NBG-18	-4.000
32	DW1303	PCEA	-5.000
31	EW0502	IG-110	-6.000
30	CW1301	H451	-7.000
29	TP25	2114	-7.625
28	FW0503	IG-430	-8.250
27	BW1403	NGB-18	-9.250
26	DW1304	PCEA	-10.250
25	EW0503	IG-110	-11.250
24	FW0504	IG-430	-12.250
23	BW1501	NGB-18	-13.250
22	1Y	Flux Monitor	-13.875
21	DW1401	PCEA	-14.500
20	FW0601	IG-430	-15.500
19	EW0504	IG-110	-16.500
18	BW1502	NBG-18	-17.500
17	DW1402	PCEA	-18.500
16	TP26	2114	-19.125
15	CW1302	H451	-19.750
14	DW18 05	PCEA	-20.375
13	M2-09	NBG-25	-20.625
12	S2 09	NBG-10	-20.875
11	FW1503	IG-430	-21.125
10	EW1403	IG-110	-21.375
9	J2 08	HLM	-21.625
8	RW4 01	BAN	-21.875
7	H572	Compact Matrix	-22.125
6	TP 20	2114	-22.375
5	L3 04	PPEA	-22.625
4	L2 10	PPEA	-22.875
3	K3 01	PGX	-23.125
2	P2-10	PCIB	-23.375

S-4, Uncompressed

Work Order 137268 Loading Order	Work Order 137268 ID Number	Graphite Type	Initial Specimen COM Elevation (in)
36	BW1602	NBG-18	-1.750
35	5B	Flux Monitor	-2.375
34	DW1502	PCEA	-3.000
33	CW202	H451	-4.000
32	AP502	NBG-17	-5.000
31	FW0604	IG-430	-6.000
30	BP602	NBG-18	-7.000
29	AL1403	NBG-17	-7.625
28	DA602	PCEA	-8.250
27	EW0604	IG-110	-9.250
26	AW1202	NBG-17	-10.250
25	CW203	H451	-11.250
24	BW1603	NBG-18	-12.250
23	DW1503	PCEA	-13.250
22	2Y	Flux Monitor	-13.875
21	EW0701	IG-110	-14.500
20	AW1203	NBG-17	-15.500
19	BP603	NBG-18	-16.500
18	DA701	PCEA	-17.500
17	FW0701	IG-430	-18.500
16	8Z	Flux Monitor	-19.125
15	EW0702	IG-110	-19.750
14	L3 05	PPEA	-20.375
13	L3 01	PPEA	-20.625
12	K3 02	PGX	-20.875
11	P3-01	PCIB	-21.125
10	DW18 06	PCEA	-21.375
9	M2-10	NBG-25	-21.625
8	S2 10	NBG-10	-21.875
7	P3-06	PCIB	-22.125
6	K3 05	PGX	-22.375
5	J2 09	HLM	-22.625
4	RW4 02	BAN	-22.875
3	H581	Compact Matrix	-23.125
2	TP21	2114	-23.375

Table 5. AGC-2 loading order for Stacks 5 and 6. (Position taken in middle of specimen or COM - Center of Mass).

S-5, Compressed

Work Order 137268 Loading Order	Work Order 137268 ID Number	Graphite Type	Initial Specimen COM Elevation (in)
23	CW301	H451	19.500
22	EW1511	IG-110	18.875
21	DW1504	PCEA	18.250
20	BW201	NBG-18	17.250
19	EW0703	IG-110	16.250
18	FW0703	IG-430	15.250
17	DW1601	PCEA	14.250
16	57	Flux Monitor	13.625
15	BW202	NBG-18	13.000
14	FW0704	IG-430	12.000
13	EW0704	IG-110	11.000
12	DW1602	PCEA	10.000
11	BW203	NGB-18	9.000
10	FW0801	IG-430	8.000
9	AW1710	NGB-17	7.375
8	CW302	H451	6.750
7	EW0801	IG-110	5.750
6	DW1603	PCEA	4.750
5	BW301	NGB-18	3.750
4	FW0802	IG-430	2.750
3	AL	Flux Monitor	2.125
2	AW1301	NGB-17	1.500

S-6, Compressed

Work Order 137268 Loading Order	Work Order 137268 ID Number	Graphite Type	Initial Specimen COM Elevation (in)
23	EW0901	IG-110	19.500
22	TP16	2114	18.875
21	FW0903	IG-430	18.250
20	DA303	PCEA	17.250
19	BP401	NBG-18	16.250
18	AW1303	NBG-17	15.250
17	EW0902	IG-110	14.250
16	5F	Flux Monitor	13.625
15	DW201	PCEA	13.000
14	BW403	NBG-18	12.000
13	CW402	H451	11.000
12	AW1401	NBG-17	10.000
11	EA902	IG-110	9.000
10	DA302	PCEA	8.000
9	TP17	2114	7.375
8	BP303	NBG-18	6.750
7	FW0904	IG-430	5.750
6	AP503	NBG-17	4.750
5	CW403	H451	3.750
4	DW202	PCEA	2.750
3	5H	Flux Monitor	2.125
2	BW501	NBG-18	1.500

S-5, Uncompressed

Work Order 137268 Loading Order	Work Order 137268 ID Number	Graphite Type	Initial Specimen COM Elevation (in)
36	AW1302	NGB-17	-1.750
35	EW1508	IG-110	-2.375
34	FW0803	IG-430	-3.000
33	BW302	NGB-18	-4.000
32	DW1604	PCEA	-5.000
31	EW0802	IG-110	-6.000
30	CW303	H451	-7.000
29	EW1507	IG-110	-7.625
28	FW0804	IG-430	-8.250
27	BW303	NGB-18	-9.250
26	DW1701	PCEA	-10.250
25	EW0803	IG-110	-11.250
24	FW0901	IG-430	-12.250
23	BW401	NBG-18	-13.250
22	7Z	Flux Monitor	-13.875
21	DW1702	PCEA	-14.500
20	FW0902	IG-430	-15.500
19	EW0804	IG-110	-16.500
18	BW402	NBG-18	-17.500
17	DW1704	PCEA	-18.500
16	EW1506	IG-110	-19.125
15	CW401	H451	-19.750
14	J2 10	HLM	-20.375
13	RW4 03	BAN	-20.625
12	H582	Compact Matrix	-20.875
11	TP 22	2114	-21.125
10	L3 06	PPEA	-21.375
9	L3 02	PPEA	-21.625
8	K3 03	PGX	-21.875
7	P3-02	PCIB	-22.125
6	DW18 07	PCEA	-22.375
5	M2-11	NBG-25	-22.625
4	S2 11	NBG-10	-22.875
3	P3-05	PCIB	-23.125
2	EW14 05	IG-110	-23.375

S-6, Uncompressed

Work Order 137268 Loading Order	Work Order 137268 ID Number	Graphite Type	Initial Specimen COM Elevation (in)
36	BW502	NBG-18	-1.750
35	TP13	2114	-2.375
34	DW203	PCEA	-3.000
33	CW501	H451	-4.000
32	AP601	NBG-17	-5.000
31	FW1001	IG-430	-6.000
30	BP302	NGB-18	-7.000
29	TP14	2114	-7.625
28	DA203	PCEA	-8.250
27	EW0904	IG-110	-9.250
26	AW1402	NBG-17	-10.250
25	CW503	H451	-11.250
24	BW503	NBG-18	-12.250
23	DW204	PCEA	-13.250
22	7Y	Flux Monitor	-13.875
21	EW1001	IG-110	-14.500
20	AW1403	NBG-17	-15.500
19	BP301	NBG-18	-16.500
18	DA202	PCEA	-17.500
17	FW1002	IG-430	-18.500
16	TP15	2114	-19.125
15	EW1002	IG-110	-19.750
14	CW14 06	H451	-20.375
13	M2-12	NBG-25	-20.625
12	S2 12	NBG-10	-20.875
11	K306	PGX	-21.125
10	EW14 06	IG-110	-21.375
9	J2 11	HLM	-21.625
8	RW4 04	BAN	-21.875
7	H591	Compact Matrix	-22.125
6	TP23	2114	-22.375
5	P3-04	PCIB	-22.625
4	L3 03	PPEA	-22.875
3	K3 04	PGX	-23.125
2	P3-03	PCIB	-23.375

Table 6. AGC-2 center channel loading order. (Position taken in middle of specimen or COM - Center of Mass)

S-7, Uncompressed			
Work Order 137268 Loading Order	Work Order 137268 ID No.	Graphite Type	Initial Specimen Elevation (in.)
170	A3P43Z12	A3 matrix	18.375
169	J1 11	HLM	18.125
168	K2 02	PGX	17.875
167	L2 01	PPEA	17.625
166	M1-12	NBG-25	17.375
165	TP 11	2114	17.125
164	P2-01	PCIB	16.875
163	RW2 02	BAN	16.625
162	S1 11	NBG-10	16.375
161	CPB101	H451	16.125
160	BP7 08	NBG-18	15.875
159	DW18 08	PCEA	15.625
158	BP7 09	NBG-18	15.375
157	FW15 04	IG-430	15.125
156	EW14 04	IG-110	14.875
155	CW14 05	H451	14.625
154	A3H08Z19	A3 matrix	14.375
153	J1 10	HLM	14.125
152	K2 01	PGX	13.875
151	L1 10	PPEA	13.625
150	M1-11	NBG-25	13.375
149	TP-10	2114	13.125
148	P1-10	PCIB	12.875
147	RW2 01	BAN	12.625
146	S1 10	NBG-10	12.375
145	CPB91	H451	12.125
144	BP7 10	NBG-18	11.875
143	DA8 05	PCEA	11.625
142	AP7 08	NBG-17	11.375
141	FW15 05	IG-430	11.125
140	EW15 03	IG-110	10.875
139	CW14 04	H451	10.625
138	H521	Compact matrix	10.375
137	J1 09	HLM	10.125
136	K1 10	PGX	9.875

Table 6. (continued).

S-7, Uncompressed			
Work Order 137268 Loading Order	Work Order 137268 ID No.	Graphite Type	Initial Specimen Elevation (in.)
135	L1 09	PPEA	9.625
134	M1-10	NBG-25	9.375
133	TP 09	2114	9.125
132	P1-09	PCIB	8.875
131	RW1 10	BAN	8.625
130	S1 09	NBG-10	8.375
129	CPB81	H451	8.125
128	BW17 01	NBG-18	7.875
127	DA8 04	PCEA	7.625
126	AP7 09	NBG-17	7.375
125	FW15 06	IG-430	7.125
124	EW15 02	IG-110	6.875
123	CW14 03	H451	6.625
122	H512	Compact matrix	6.375
121	J1 08	HLM	6.125
120	K1 09	PGX	5.875
119	L1 08	PPEA	5.625
118	M1-09	NBG-25	5.375
117	TP 08	2114	5.125
116	P1-08	PCIB	4.875
115	RW1 09	BAN	4.625
114	S1 08	NBG-10	4.375
113	CPB71	H451	4.125
112	BW17 09	NBG-18	3.875
111	DA8 03	PCEA	3.625
110	AP7 10	NBG-17	3.375
109	FW16 01	IG-430	3.125
108	EW15 01	IG-110	2.875
107	CPB151	H451	2.625
106	A3P33Z09	A3 matrix	2.375
105	J1 07	HLM	2.125
104	K1 08	PGX	1.875
103	L1 07	PPEA	1.625
102	M1-08	NBG-25	1.375
101	TP 07	2114	1.125
100	P1-07	PCIB	0.875
99	RW1 08	BAN	0.625
98	S1 07	NBG-10	0.375

Table 6. (continued).

S-7, Uncompressed			
Work Order 137268 Loading Order	Work Order 137268 ID No.	Graphite Type	Initial Specimen Elevation (in.)
97	CPB61	H451	0.125
96	BW17 08	NBG-18	−0.125
95	DA8 02	PCEA	−0.375
94	AW17 01	NBG-17	−0.625
93	FW15 12	IG-430	−0.875
92	EW14 12	IG-110	−1.125
91	CPB141	H451	−1.375
90	A3H08Z07	A3 matrix	−1.625
89	J1 06	HLM	−1.875
88	K1 07	PGX	−2.125
87	L1 06	PPEA	−2.375
86	M1-07	NBG-25	−2.625
85	TP 06	2114	−2.875
84	P1-06	PCIB	−3.125
83	RW1 07	BAN	−3.375
82	S1 06	NBG-10	−3.625
81	CPB51	H451	−3.875
80	BW17 07	NBG-18	−4.125
79	DA8 01	PCEA	−4.375
78	AW17 02	NBG-17	−4.625
77	FW15 11	IG-430	−4.875
76	EW14 11	IG-110	−5.125
75	CPB131	H451	−5.375
74	A3P43Z03	A3 matrix	−5.625
73	J1 05	HLM	−5.875
72	K1 06	PGX	−6.125
71	L1 05	PPEA	−6.375
70	M1-06	NBG-25	−6.625
69	TP 05	2114	−6.875
68	P1-05	PCIB	−7.125
67	RW1 06	BAN	−7.375
66	S1 05	NBG-10	−7.625
65	CPB41	H451	−7.875
64	BW17 05	NBG-18	−8.125
63	DW18 12	PCEA	−8.375
62	AW17 03	NBG-17	−8.625
61	FW15 10	IG-430	−8.875
60	EW14 10	IG-110	−9.125

Table 6. (continued).

S-7, Uncompressed			
Work Order 137268 Loading Order	Work Order 137268 ID No.	Graphite Type	Initial Specimen Elevation (in.)
59	CPB121	H451	−9.375
58	H491	Compact matrix	−9.625
57	J1 04	HLM	−9.875
56	K1 05	PGX	−10.125
55	L1 04	PPEA	−10.375
54	M1-05	NBG-25	−10.625
53	TP 04	2114	−10.875
52	P1-04	PCIB	−11.125
51	RW1 05	BAN	−11.375
50	S1 04	NBG-10	−11.625
49	CPB31	H451	−11.875
48	BW17 04	NBG-18	−12.125
47	DW18 11	PCEA	−12.375
46	AW17 06	NBG-17	−12.625
45	FW15 09	IG-430	−12.875
44	EW14 09	IG-110	−13.125
43	CPB111	H451	−13.375
42	H482	Compact matrix	−13.625
41	J1 03	HLM	−13.875
40	K1 04	PGX	−14.125
39	L1 03	PPEA	−14.375
38	M1-04	NBG-25	−14.625
37	TP-03	2114	−14.875
36	P1-03	PCIB	−15.125
35	RW1 04	BAN	−15.375
34	S1 03	NBG-10	−15.625
33	CPB21	H451	−15.875
32	BW17 03	NBG-18	−16.125
31	DW18 10	PCEA	−16.375
30	AW17 05	NBG-17	−16.625
29	FW15 08	IG-430	−16.875
28	EW14 08	IB-110	−17.125
27	CA11 02	H451	−17.375
26	A3P33Z20	A3 matrix	−17.625
25	J1 02	HLM	−17.875
24	K1 03	PGX	−18.125
23	L1 02	PPEA	−18.375
22	M1-02	NBG-25	−18.625

Table 6. (continued).

S-7, Uncompressed			
Work Order 137268 Loading Order	Work Order 137268 ID No.	Graphite Type	Initial Specimen Elevation (in.)
21	TP 02	2114	−18.875
20	P1-02	PCIB	−19.125
19	RW1 03	BAN	−19.375
18	S1 02	NBG-10	−19.625
17	CPB11	H451	−19.875
16	BW17 02	NBG-18	−20.125
15	DW18 09	PCEA	−20.375
14	AW17 04	NBG-17	−20.625
13	FW15 07	IG-430	−20.875
12	EW14 07	IG-110	−21.125
11	CA11 01	H451	−21.375
10	H472	Compact matrix	−21.625
9	J1 01	HLM	−21.875
8	K1 01	PGX	−22.125
7	L1 01	PPEA	−22.375
6	M1-01	NBG-25	−22.625
5	TP 01	2114	−22.875
4	P1-01	PCIB	−23.125
3	RW1 02	BAN	−23.375
2	CPB1	H451	−23.625
1	S101[a]	NBG-10	−23.875
a. Note: Specimen S101 (grade NBG-10) was lost during the disassembly of the AGC-2 irradiation capsule.			

Following irradiation in the ATR at INL, the AGC-2 capsule was disassembled.[23,24] All specimens recovered from disassembly were visually inspected and physically measured within the INL Carbon Characterization Laboratory before being stored in the irradiated graphite storage vault. It should be noted that NBG-25 Specimen S101 was lost (missing) during AGC-2 disassembly activities.[23] After accounting for all recovered specimens from the AGC-2 capsule, PIE and testing were performed for each specimen at the INL Carbon Characterization Laboratory.

4. AGC-2 AS-RUN IRRADIATION CONDITIONS

AGC-2 was designed to provide irradiation conditions similar to AGC-1 (i.e., the same graphite grades, a nominal irradiation temperature of 600°C, and the same applied mechanical loading) but was irradiated for a shorter period of time to provide material property values for the graphite samples at lower dose levels than those achieved in AGC-1. An additional objective was to implement capsule design improvements learned from AGC-1 to reduce the large specimen temperature range experienced in AGC-1.

AGC-2 was irradiated in the south flux trap of ATR between April 12, 2011, and May 5, 2012.[18,23] AGC-2 was irradiated over five reactor cycles, Cycles 149A, 149B, 150B, 151A, and 151B (there was no Cycle 150A), for a total of 5,539 MW days or approximately 230 effective full power days. The final specimen dose levels ranged from 2.0–4.7 dpa with the specimens at the mid-plane elevation receiving the highest accumulated dose levels.[25]

Irradiation creep is defined as the difference in dimensional change between stressed (creep) and unstressed (control) samples irradiated at similar dose and temperature levels. To induce irradiation creep strain within the AGC-2 creep specimens, one half of the specimens were subjected to mechanical stresses while the remainder of the specimens had no applied stresses. Stressed samples were subjected to three different stresses: a nominal stress of 13.8 MPa for specimens in Stacks 1 and 4, 17.2 MPa for Stacks 2 and 5, and the highest nominal stress of 20.7 MPa for the 12.7 mm (0.5-in.) diameter specimens in Stacks 3 and 6.

Stress level changes resulting from specimen lateral shrinkage or expansion during irradiation were ignored.[26] The total applied stress levels over all irradiation cycles were demonstrated to be relatively constant for all stack loading and consistent between similar loaded stacks (Table 7). The coefficient of variation of applied stress to all stacks (the extent of variability to the mean of all applied stresses) is ~1% across the entire AGC-2 irradiation.

Table 7. Load values after application of threshold for each stack.

	Stack 1	Stack 2	Stack 3	Stack 4	Stack 5	Stack 6
Average (MPa)	14.3	17.8	21.3	13.9	17.7	21.2
Two times standard deviation (MPa)	0.4	0.5	0.4	0.3	0.2	0.4
Coefficient of variance (%)	1.3	1.3	1.0	1.1	0.7	0.8

Modifications to AGC-2 capsule design were primarily intended to reduce the range of specimen temperatures, because it is desired that all specimens be irradiated as close to 600°C as possible. The AGC-2 creep and control specimen temperatures ranged from 541– 681°C,[27,28] which was markedly better than the AGC-1 specimens (with a range of 468 - 716 °C),[17,29,30] but it is still considered less than optimal as defined for AGC-2 capsule irradiation specifications (average capsule temperature maintained at 600°C ±50°C).[5] A detailed uncertainty analysis of the temperature model used to derive the specimen temperatures yields a maximum uncertainty of ±40°C for the individual AGC-2 specimen temperatures.[31] Maximum and minimum temperatures between stacks were significantly improved (maximum

temperature range of 666–681°C and minimum temperature range of 541–553°C) as were temperatures between AGC-2 matched-pair specimens.

5.   CREEP STRAIN DATA

Dimensional change (strain) data for all major graphite grades are provided in INL's "AGC-2 Specimen Post-Irradiation Data Package Report".[4] The total specimen irradiation dose, average irradiation temperature, and applied mechanical load during irradiation for each specimen are recorded along with the dimensional change measurements. Total volumetric, length, and diametric dimensional AGC-2 specimen changes are summarized in Figure 5 through Figure 7 for the control specimens and three applied mechanical load states. It should be noted that volume, length and diameter changes are strongly related to the irradiation temperature and received dose, as will be discussed further in later sections. These figures, demonstrating dimensional change effects from the applied mechanical load, are meant to compare the mean values of the total dimensional and volume variables between grades.
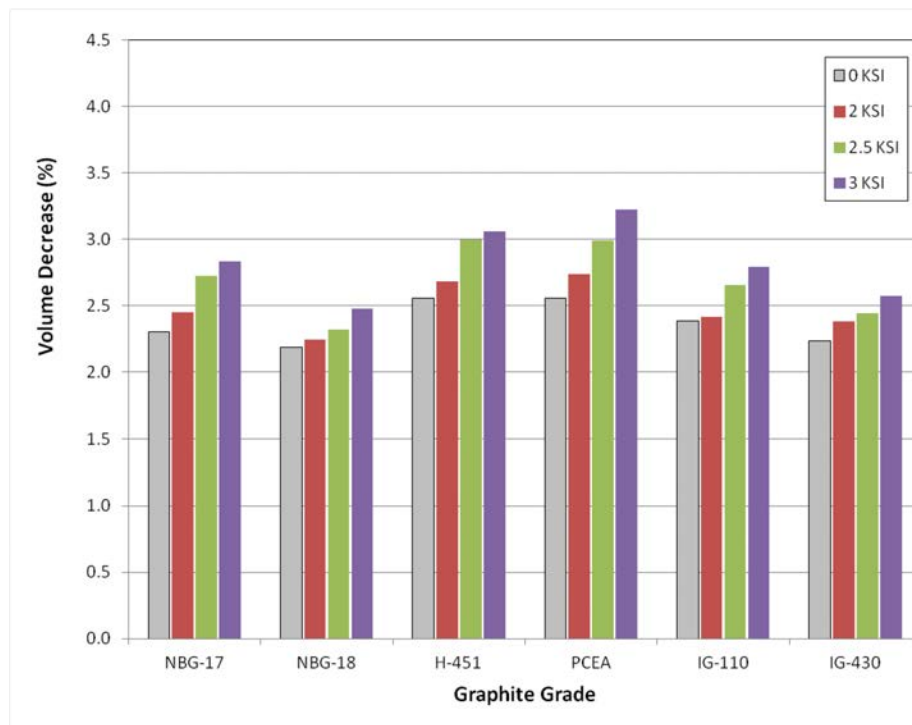

Figure 5. Total maximum volume decrease (%) due to irradiation creep for six major grades of graphite. The dimensional change dependency on irradiation dose and irradiation temperature is not presented.
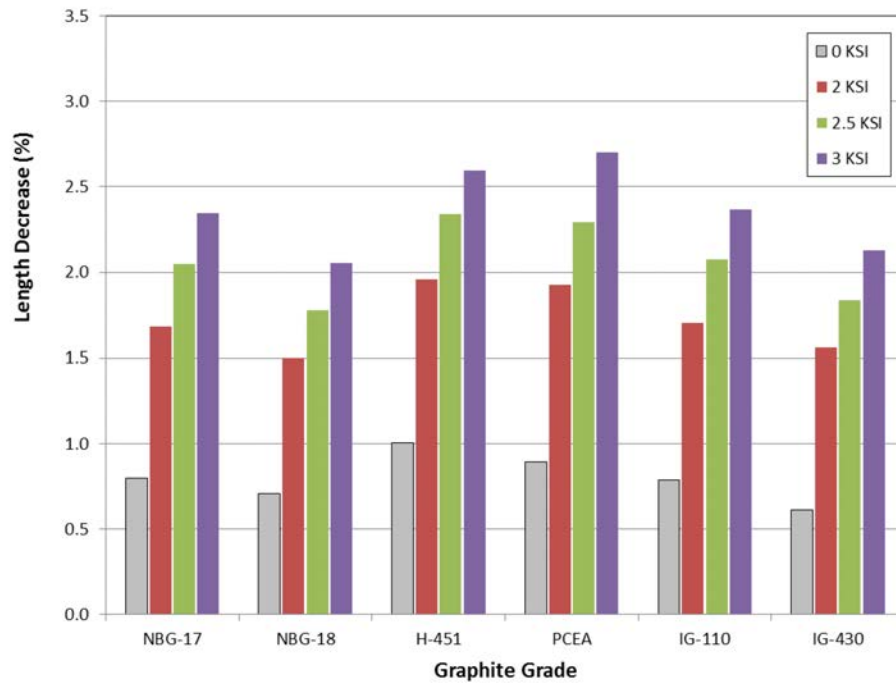
Figure 6. Average length decrease (%) at maximum dose received for six major grades of graphite. The dimensional change dependency on irradiation dose and irradiation temperature is not presented.
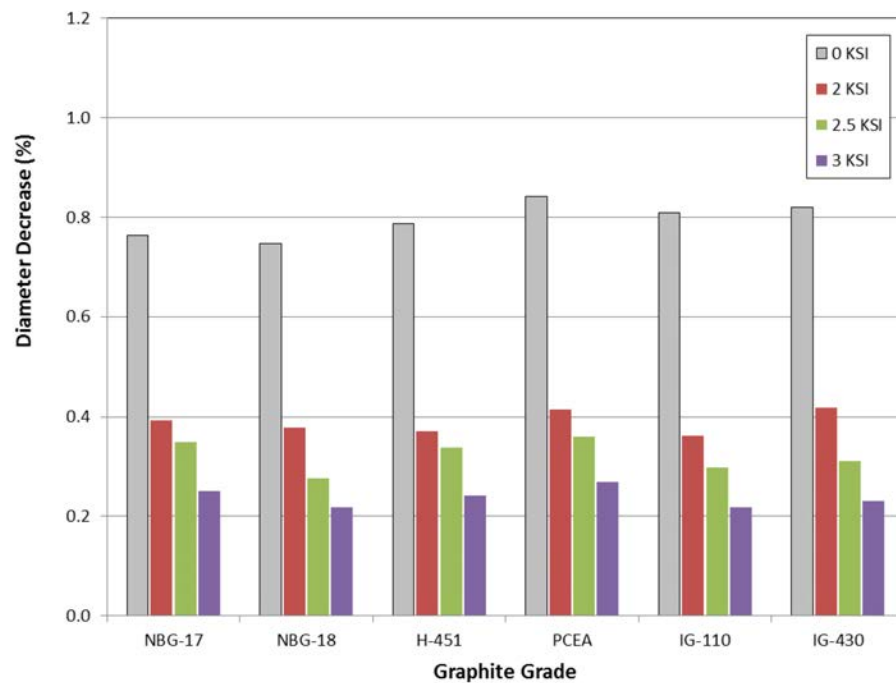

Figure 7. Total maximum diameter decrease (%) due to irradiation creep for six major grades of graphite. Note the diameter decrease in stressed (creep) samples was lower than unstressed (control) samples due to "barreling" effects mitigating the shrinkage (note: barreling produced a variety of out-of-round shapes,

including hourglass, pear, and the simple barrel shape). The dimensional change dependency on irradiation dose and irradiation temperature is not presented.

The underlying mechanisms responsible for irradiation-induced creep in graphite are still relatively unknown. Traditionally, irradiation creep of graphite is defined as the macroscopic dimensional change in a specimen occurring under the simultaneous influence of neutron irradiation and mechanical stresses. Stresses sufficiently large enough to cause irradiation creep are induced in the graphite microstructure by large temperature and/or neutron flux gradients through the large reactor components. Irradiation creep is fluence dependent (i.e. time in reactor) at temperatures well below where thermal creep would normally be observed in a graphite specimen.

Conventionally, this phenomenon has been studied experimentally in material test reactors on small graphite specimens kept at a constant mechanical load. The apparent creep strain is determined by comparing the irradiation-induced dimensional changes (strains) in specimens irradiated under identical conditions, but where one specimen is mechanically loaded (creep specimen) and the other specimen is not (the control specimen). The difference between the dimensional change of the creep and control specimen yields the creep strain. While all graphite specimens will experience dimensional change, the mechanically loaded specimens will experience different strain values than the matching unstressed specimens, yielding a value for the irradiation induced creep strain.

Creep experiments of this nature, with both tensile and compressive applied stresses, have been performed in previous studies across a relatively large neutron dose range. Generally, three stages of graphite irradiation creep are recognized (Figure 8):

- Stage I: In the first stage of creep, initial strain accumulates rapidly with dose but quickly saturates to a strain level of one elastic strain unit defined as $\sigma_{(applied)}/E_0$, where $\sigma_{(applied)}$ is the applied mechanical stress to the specimen and E_0 is the unirradiated Young's modulus value of the stressed specimen. Stage I creep is referred to as "primary creep" and occurs at very low dose level, <1 dpa.

- Stage II: In the second stage, accumulation of creep strain that is linearly proportional to the neutron dose and applied stress. Stage II creep is referred to as "steady-state creep" or "linear creep." The slope of a plot of second-stage, or secondary, creep strain should be a straight line with slope K, the creep coefficient. Typically, this stage is dominant between 1 and 10 dpa for most graphite grades, but the dose range over which secondary creep occurs is temperature and graphite grade dependent. Previous studies have demonstrated that Stage II creep (linear accumulation of strain) stops when dimensional volume change turnaround has been achieved.

- Stage III: The third and final stage is a nonlinear acceleration of accumulated creep strain that usual occurs after dimensional volume change turnaround. Stage III occurs at higher doses, typically >10 dpa, where the rate of accumulation of irradiation creep strain accelerates with dose.

Creep Strain, %

Stage I ⋮ Stage II ⋮ Stage III

Gradient = Liner stage
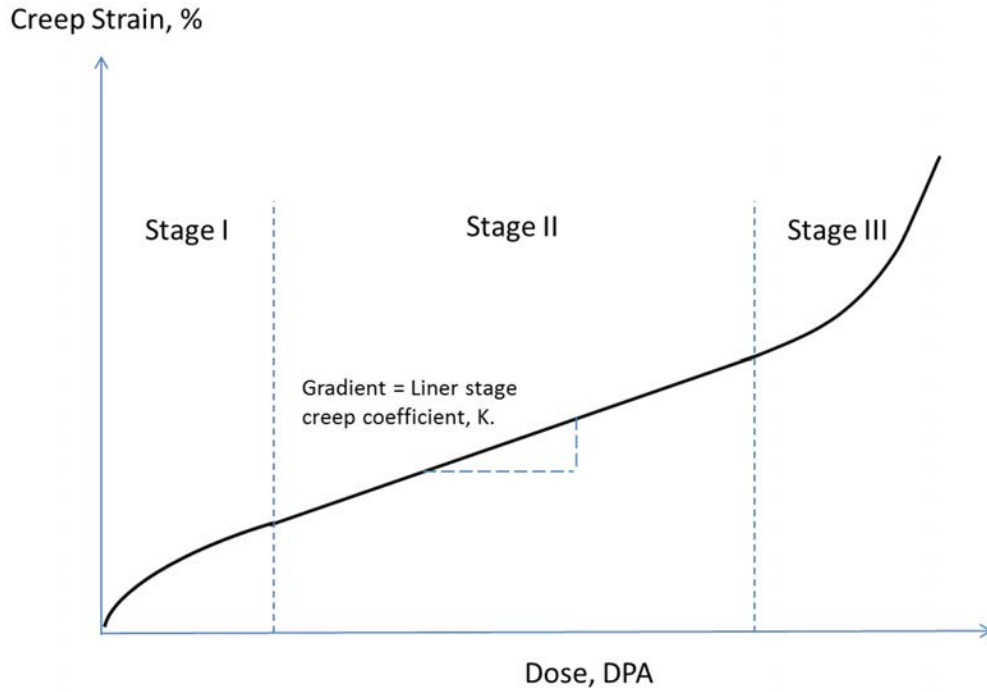creep coefficient, K.

Dose, DPA

Figure 8. A schematic representation of the three stages of irradiation-induced creep.

Creep during Stages I and II are thought to be dominated by dislocation formation and flow processes (i.e., primarily in-crystal effects only). Whereas Stage III creep (which occurs at higher doses, after the point of volume change turnaround) is thought to be related to graphite structure changes (i.e., both in-crystal and pore volume effects). Additional irradiation-induced creep strain data are required for the development of a more complete understanding of the underlying mechanisms responsible for graphite creep.

The AGC-2 experiment was designed to operate in Stage II, where dose and irradiation temperature produce a linear accumulation of creep strain. Previous studies have developed a viscoelastic creep law that applies to this linear stage of creep (Figure 8).[32,33,34,35] Under the linear viscoelastic creep law, the normalized secondary creep data are shown to be linear, indicating no structure effects at these (lower) doses. This report uses this linear relationship to obtain the total creep strain for the AGC-2 specimens with the following relationship:

$$\varepsilon_{c(TOTAL)} = \varepsilon_{cPRIMARY} + \varepsilon_{cSECONDARY} \, (\%)$$

$$\varepsilon_{cPRIMARY} = \frac{A\sigma}{E_0}[1 - Exp(-b\gamma)] \approx \frac{\sigma}{E_0} \, (\%)$$

$$\varepsilon_{cSECONDARY} = K\sigma\gamma \, (\%)$$

$$\varepsilon_{c(TOTAL)} = \frac{\sigma}{E_0} + K\sigma\gamma \, (\%)$$

where

K = K'/σ_{max} = secondary creep constant in % change/(dpa·MPa) or 10^{-30}cm^2/(n·Pa)

σ = applied stress (MPa)

γ   =   neutron dose (dpa)

E_0 =   initial (pre-irradiation) Young's modulus of stressed specimen with A and b as fitting constants to the primary creep equation.

Applying this viscoelastic creep law relationship to the AGC-2 data allows the creep coefficient, K, to be calculated from the measured dimensional change data for each graphite grade. The methodology and calculations for calculating the creep coefficient are described in the following section.

6.   CREEP STRAIN ANALYSIS METHODOLOGY

Similar to the AGC-1 analysis, AGC-2 creep strain analysis and comparisons will be made between the AGC-2 historic grade of graphite (H-451) and prior H-451 data, including the past H-451 data from AGC-1. In addition, comparisons are made between the two vibrationally molded grades (NBG-18 and NBG-17), the extruded graphite grades (H-451 and PCEA), and the two isostatically molded grades (IG-110 and IG-430). The creep strain analysis methodology for AGC-2 is nearly identical to the AGC-1 analysis and is described in detail in *AGC-1 Irradiation Creep Strain Data Analysis*.[29] Using this established outline, a semi-automated spreadsheet was developed to provide for an efficient and accurate method to calculate the creep coefficient as a function of the AGC irradiation variables. The spreadsheet is also envisioned to enable comparisons of different combinations of AGC creep data with future irradiation capsules (i.e., AGC-3, AGC-4, etc.).

6.1   Methodology Steps

A diagram representing the AGC-2 Creep Strain Rate Calculation Spreadsheet data flow (Figure 9) illustrates the seven input data streams (i.e., input tabs) necessary to calculate the creep coefficient. The input tabs are populated with data from specimen property measurements[4,20,22] or capsule irradiation data[18,25,26,27, 28] that are needed to perform creep strain calculations on individual specimen matched pairs. Once the data streams have been established and verified, the calculations are performed for each matched pair.

Gathering and sorting the specific data required for all matched pairs within an AGC irradiation capsule is complicated. A separate subroutine (i.e., Lookup Tab) was specifically developed to identify the matching pair for each creep specimen, gather the specific pre- and post-irradiated material properties for each specimen needed for creep calculations, and apply the appropriate irradiation conditions for each matched pair. This data collation is performed by utilizing each individual specimen identification number to gather all of the pertinent data for each specific specimen, including specimen pre-irradiation elastic moduli (acquired via both the sonic resonance and the sonic velocity methods), pre- and post-irradiation dimensional measurements, irradiation temperature, applied stress, dose, elevational analysis, and matched-pair identification to populate the input tabs.
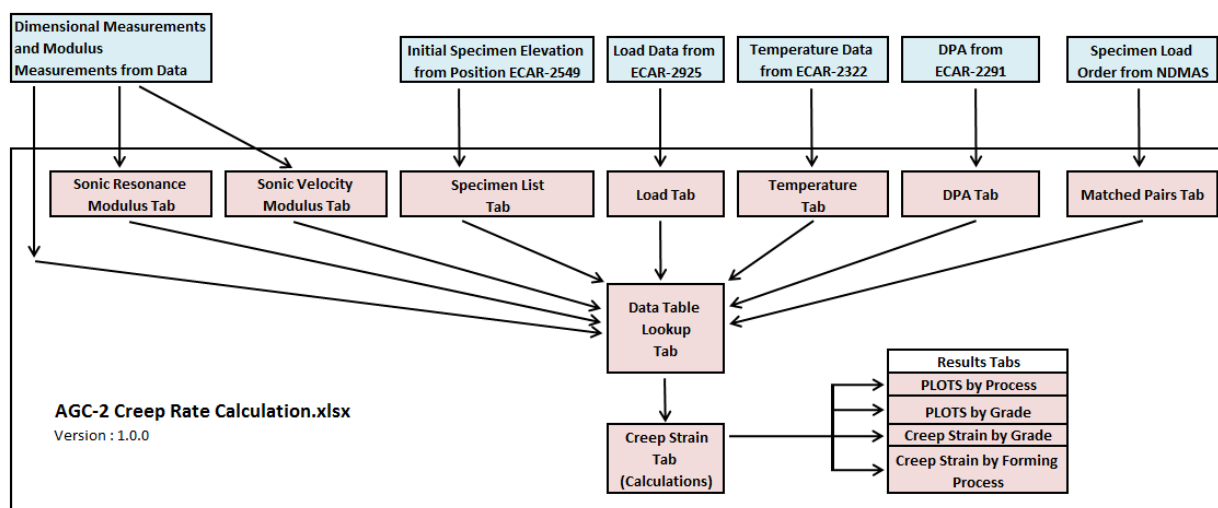
Figure 9. Data flow of AGC-2 Creep Rate Calculation Spreadsheet.

Creep strain is calculated (i.e., Calculate Tab) from the compiled data for every specimen and every graphite grade using the viscoelastic creep law relationship and the methodology developed in AGC-1 creep analysis.[29] The spreadsheet generates either data plots or tables of the creep strain after calculation. Currently, the output results can be sorted by grade or fabrication process (i.e., Results Tab) in order to easily compare the results for similar grades. Further sorting capabilities can be added as needed. Finally, the spreadsheet also allows for data filtering that can be used to limit the specimens considered in the calculation to those within a specified temperature and/or dose range. Following input data insertion, the appropriate spreadsheet cells are locked to prevent inadvertent deletion or modification of data or formulas.

Results from spreadsheet calculations were independently validated by manually preforming creep strain calculations through an independent reviewer. The results of this acceptance testing and the spreadsheet's software management plan are documented using INL Form 562.41, "Software Management Plan and Life Cycle Documentation for Research and Development Activities" (07/01/2015, Rev. 00). This is retrievable by searching for "AGC-2 Creep Rate Calculation Spreadsheet" in INL's Electronic Document Management System.[36]

7. DIMENSIONAL CHANGE ANALYSIS

Before creep strain results are calculated it is useful to investigate the dimensional change behavior of the major AGC-2 graphite grades. Dimensional changes (longitudinal, lateral, and volumetric) can provide insights into the isotropic material response, diametral/longitudinal irradiation response, and volumetric conservation of the grades after being irradiated.

7.1 Confirming AGC-2 Dimensional Change Behavior

Unstressed irradiated dimensional change behavior of the AGC-2 historical grade, H-451, is compared to historical H-451 specimen data from prior irradiated H-451 studies (Figure 10). The AGC-2 results match well with previous measured strains for unstressed control H-451 specimens in the longitudinal and lateral directions, demonstrating the validity of the AGC irradiation parameters and experimental conditions. The secondary creep strain is linear, allowing a constant creep strain rate to be calculated for the dose and temperature range of AGC-2.
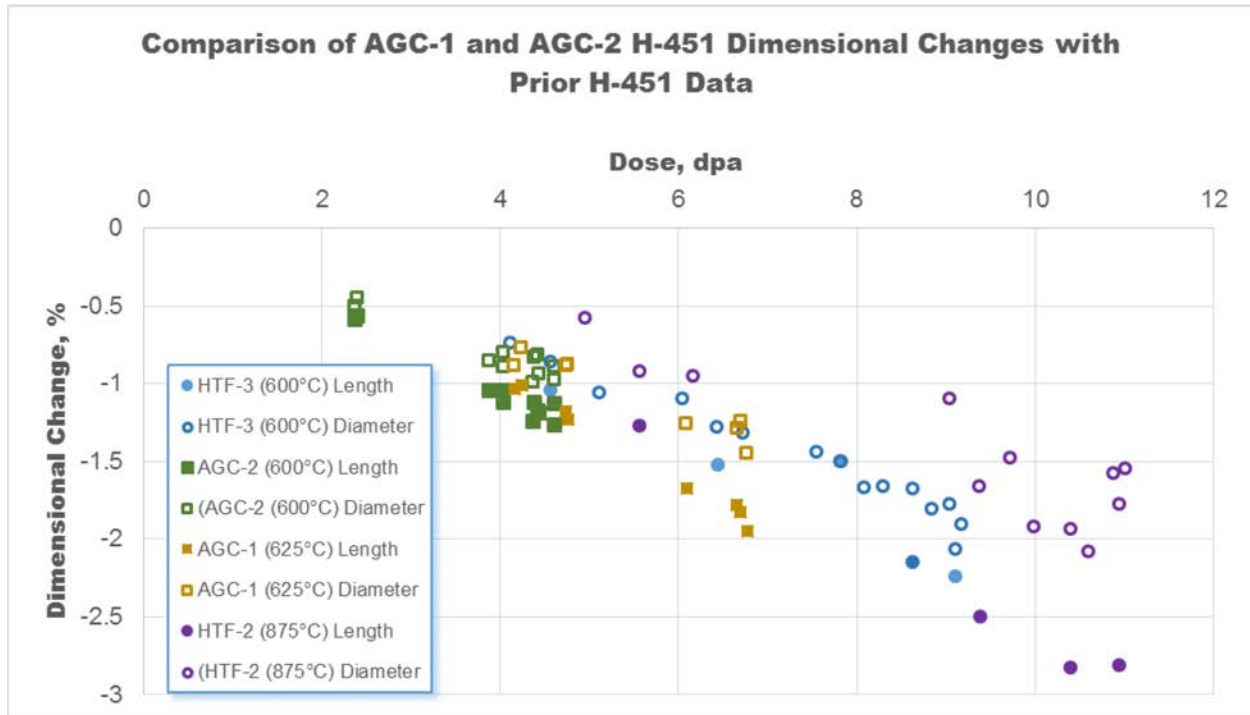
Figure 10. Comparison of AGC-2 historical grade (H-451) dimensional changes to previous H-451 specimens irradiated in AGC-1 and prior graphite creep studies.

7.2   Dimensional Change Analysis by Graphite Grade

After establishing the validity of the AGC experimental parameters it is instructional to analyze the dimensional irradiation response for all major grades of graphite in AGC-2. The dimensional change behavior can provide insights into the isotropic material response, diametral and/or longitudinal irradiation response, or whether a grade is approaching turnaround, as well as other behaviors.

The dimensional changes over the AGC-2 dose range for all major AGC-2 graphite grades are summarized from pre- and post-irradiation specimen measurements. Plotting dimensional behavior of the unstressed control specimen length and diameter changes illustrates the isotropic irradiation response of the graphite. Because no additional mechanical stresses are involved, it can be assumed that the irradiation-induced stress within the graphite specimens is isostatic, creating similar dimensional change behavior in both lateral and longitudinal directions. The dimensional behavior is grouped by graphite fabrication process (i.e., vibrationally molded, extruded, isostatically molded) to illustrate the irradiation induced similarities and differences between the various grades (Figure 11, Figure 12, and Figure 13).
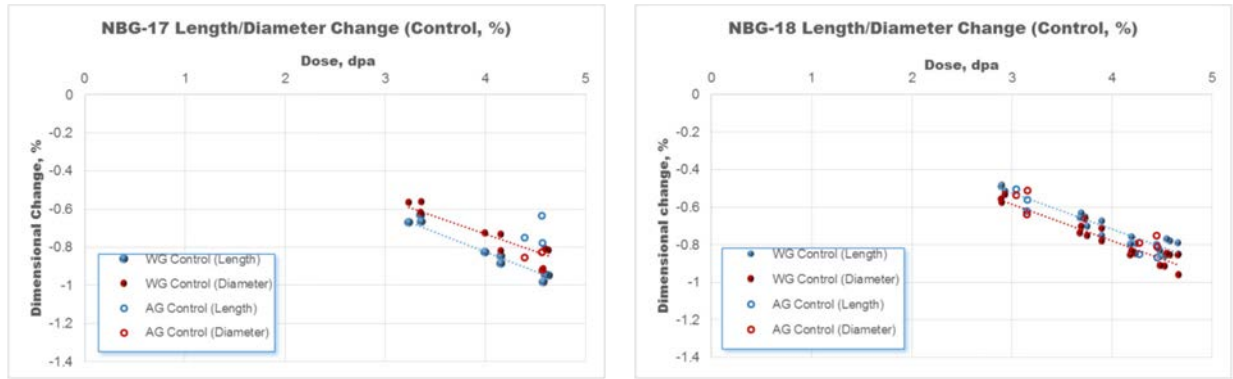
28

Figure 11. Comparison of dimensional change in longitudinal and diametral directions for NBG-17 and NBG-18 unstressed control specimens. Data points designated as O indicate AG specimens.
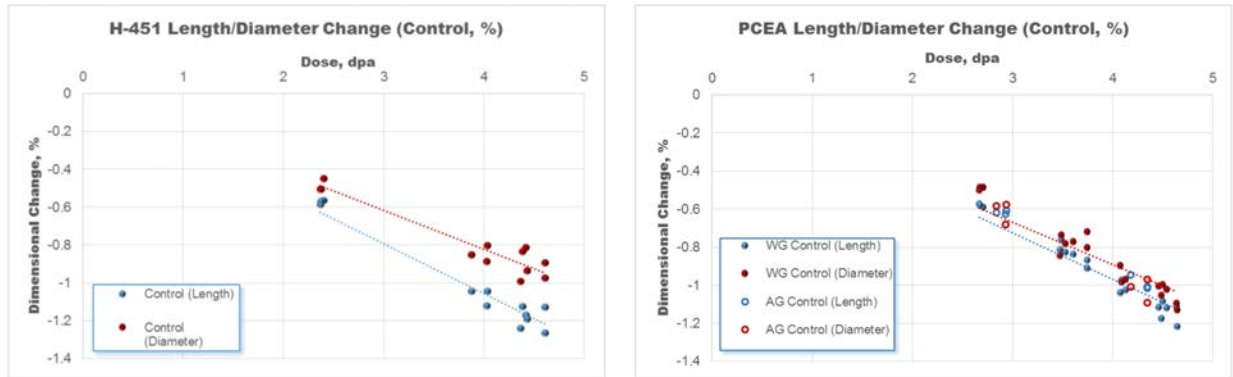

Figure 12. Comparison of dimensional change in longitudinal and diametral directions for H-451 and PCEA unstressed control specimens. Data points designated as O indicate AG specimens.
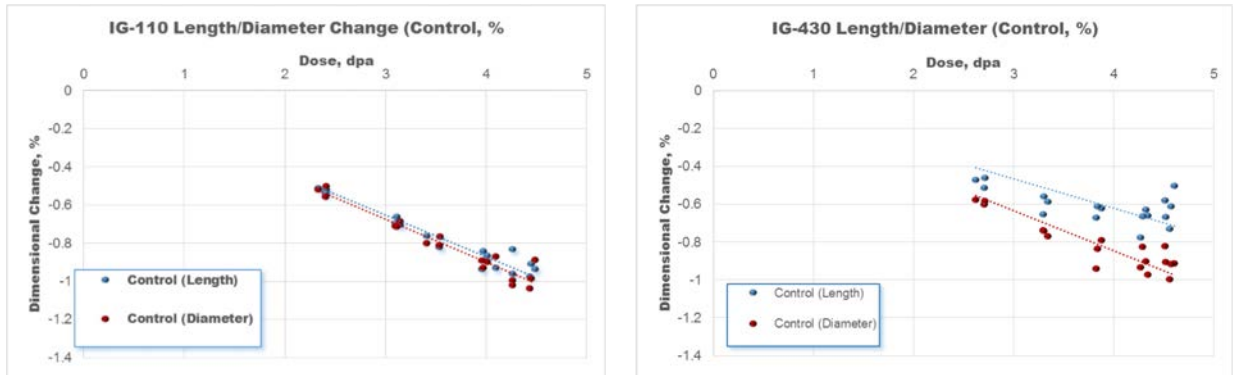

Figure 13. Comparison of dimensional change in longitudinal and diametral directions for IG-110 and IG-430 unstressed control specimens. Isostatic molded grades do not have a WG or AG structure, so specimens are not included.

Isotropic graphite should have identical dimensional change in all directions (i.e., an isotropic response). All AGC-2 specimens show isotropic or near-isotropic responses over the dose and temperature range of AGC-2 irradiation conditions, with IG-110 clearly demonstrating complete isotropic response and IG-430 having the least isotropic response. It should be noted that AG and WG specimens had a nearly identical response, again demonstrating near-isotropic response for those major graphite grades.

Graphite grades IG-110, NBG-17, NBG-18, and PCEA showed the most isotropic response (i.e., lowest variation between length and diameter change). While this response is not surprising for the isostatically formed IG-110, it is unexpected for the extruded PCEA. Both WG and AG specimen response is effectively the same for length and diameter change for PCEA. It should be noted that the three AG length measurements for NBG-17 appear to show a larger variation than the WG length measurements.

H-451 and IG-430 show the widest variation between length and diameter dimensional change. While this response is expected with the extruded H-451 grade, which can produce some textured microstructure due to extrusion fabrication, it is surprising for the isostatically formed IG-430. Finally, IG-430 shows higher overall dimensional change variability at higher dose levels. This variability in IG-430 at higher dose levels was experienced in AGC-1 as well. At this time, no firm conclusions can be derived from the IG-430 behavior.

Any change in isotropy from irradiation, as determined through changes in Poisson's ratio, will be investigated in a future AGC-2 irradiated material analysis. These data trends will be compared to the results from Poisson's ratio changes.

7.3   Volume Change Analysis by Graphite Grade

The volume change behavior for each graphite grade is calculated from the specimen pre-irradiation examination and PIE dimensional measurements and summarized in Figure 14, Figure 15, and Figure 16. All grades exhibited linear volumetric change, with the extruded grades showing the largest decrease. All vibrationally and isostatically molded grades had similar levels of volumetric decrease. This trend extends to samples where the compressive load was applied in the AG direction of the grade. As seen, the AG and WG specimens had similar volume change behavior.
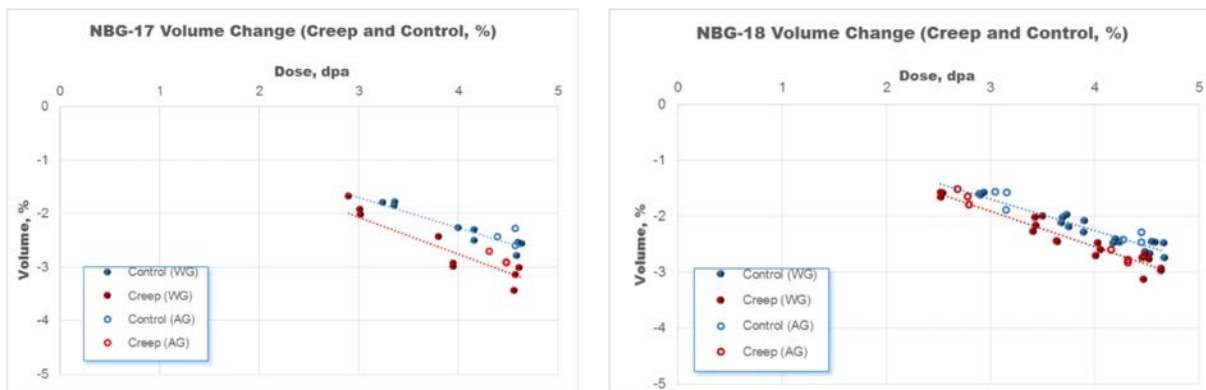

Figure 14. Volume changes of vibrationally molded graphite grades NBG-17 and NBG-18 for creep and control specimens. Data points designated as ○ indicate AG specimens.
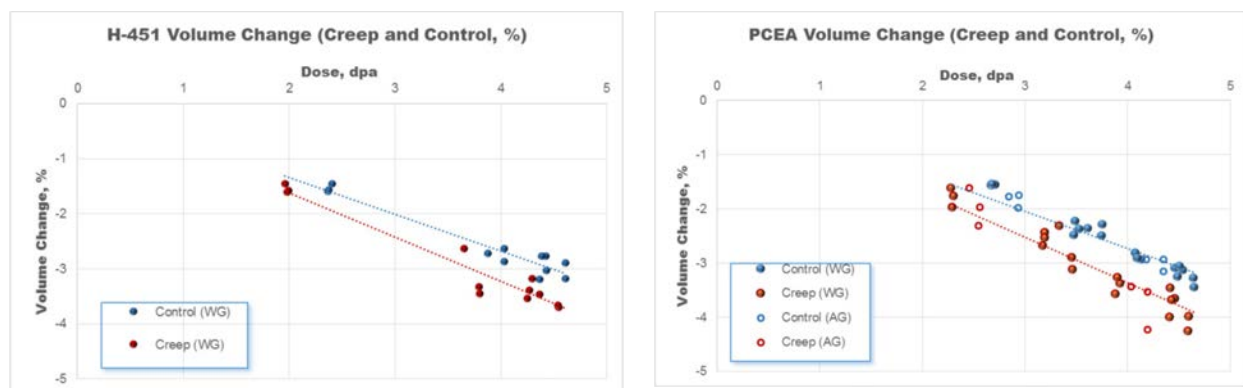
Figure 15. Volume change of extruded graphite grades H-451 and PCEA for both creep and control specimens. Data points designated as O indicate AG specimens. No AG H-451 specimens were included in AGC-2.
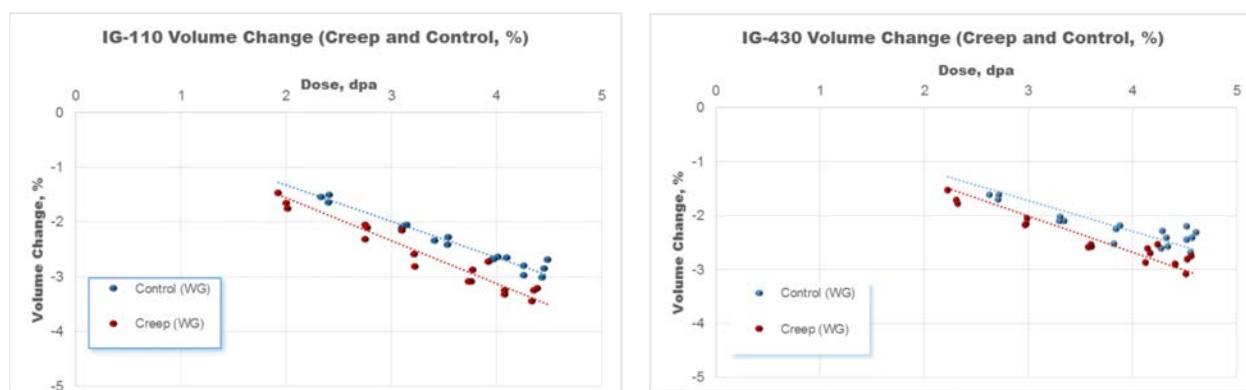

Figure 16. Volume change of isostatically molded graphite grades IG-110 and IG-430 for creep and control specimens. Isostatic grades do not have a WG or AG grain structure, so specimens are not included.

While all grades exhibited similar dimensional change behavior, there was a measurable difference between creep (stressed) and control (unstressed) specimens. The largest differences between creep and control specimens were for the extruded grades, H-451 and PCEA (i.e., ~ 1% maximum), and NBG-17 (i.e., ~1% maximum). The two isostatically molded grades, IG-110 and IG-430, as well as NBG-18 experienced essentially the same response for creep and control specimens. This data trend for IG-430 is slightly suspect due to the high variability demonstrated for the higher dose levels, as seen in Figure 16.

So while some of the AGC-2 grades demonstrate similar volumetric changes for creep and control conditions other grades do not. Since creep specimens are exposed to mechanical loads and experience higher strain levels than unstressed control specimens, this variation implies that the lateral strain in the creep specimens must be accounting for the volume conservation in the grades with similar volume changes. It should be noted that the volume calculations rely on the diameter measurements, and these measurements have been shown to have significantly higher data scatter levels, which can affect this conclusion. So, while some grades demonstrate volume conservation it is not universally seen for all AGC-2 graphite grades. This is a slight discrepancy from the AGC-1 analysis, which showed evidence of volume change for all graphite grades and will require further investigation in future AGC irradiations.

8.   CREEP ANALYSIS

Longitudinal and lateral creep strain are calculated from the difference between the creep and control specimen lengths and diameters, respectively. AGC-2 creep calculations for all major graphite grades were performed using the AGC-2 Creep Rate Calculation Spreadsheet. For these relatively lower dose levels (<10 dpa), the creep response should be linear and proportional to the applied stress, implying that a larger stress will induce more strain, resulting in a steeper slope to the calculated creep curve. The creep specimens are subjected to a compressive stress, which will yield a negative slope to the longitudinal creep curve. However, the lateral creep strain response should be positive, because it results from the Poisson's stress, which yields an outward tensile force to the specimen sides and creates an induced lateral tensile strain orthogonal to the applied longitudinal stress (i.e., the Poisson's effect, which pushes the sides of the specimen outward).

8.1   Creep Analysis by Graphite Grade

Examples of the calculated strain response are presented by creep strain for the major AGC-2 graphite grades in Figure 17 through Figure 22. The data are plotted over the AGC-2 irradiation temperatures (541–681°C), dose range (2.0–4.7 dpa) and at the three applied mechanical load levels, which are represented as three different sized filled circles. In an attempt to discriminate between dimensional changes at different temperatures, the data are color coded to illustrate the irradiation temperature for each specific data point. The temperatures are roughly divided into 25°C increments over the total creep specimen irradiation temperature range.

In addition, AG specimens are represented by hollow circles. NBG-17 data points with a black outline (either solid or hollow) are NBG-17 specimens with a low density.[20] These low-density specimens were purposely added to the AGC-2 irradiation capsule to ascertain what, if any, changes to the bulk density may have on the irradiation behavior of graphite.
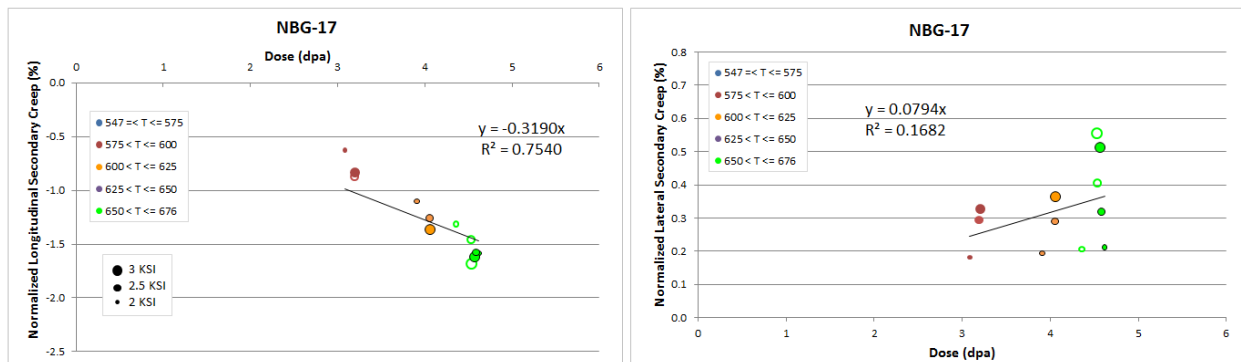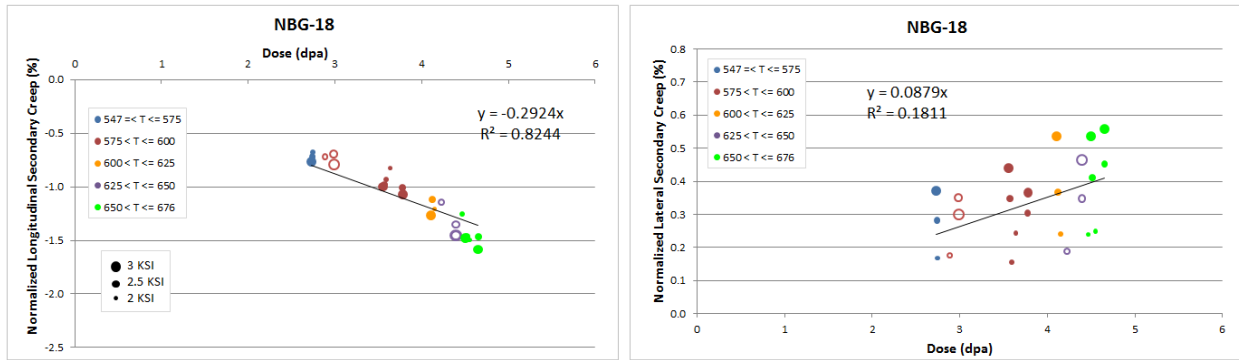

Figure 17. Longitudinal and lateral secondary creep for grade NBG-17 as calculated from the AGC-2 Creep Rate Calculation Spreadsheet. Results are calculated over the entire AGC-2 temperature (541–681°C) and three stress levels (• = 13.8 MPa, • = 17.2 MPa, • = 20.7 MPa). Note the data points with black outlines represent low density NBG-17 specimens.

Figure 18. Longitudinal and lateral secondary creep for grade NBG-18 as calculated from the AGC-2 Creep Rate Calculation Spreadsheet. Results are calculated over the entire AGC-2 temperature (541–681°C) and three stress levels (• = 13.8 MPa, • = 17.2 MPa, • = 20.7 MPa).
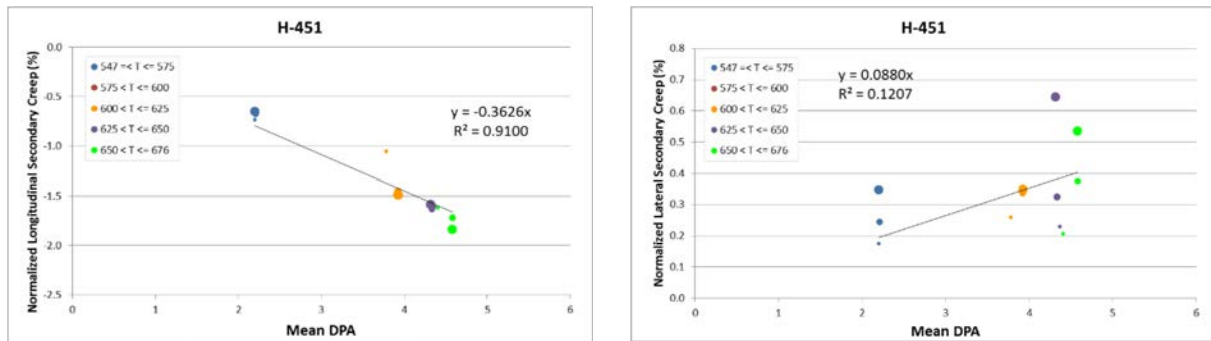

Figure 19. Longitudinal and lateral secondary creep for grade H-451 as calculated from the AGC-2 Creep Rate Calculation Spreadsheet. Results are calculated over the entire AGC-2 temperature (541–681°C) and three stress levels (• = 13.8 MPa, • = 17.2 MPa, • = 20.7 MPa).
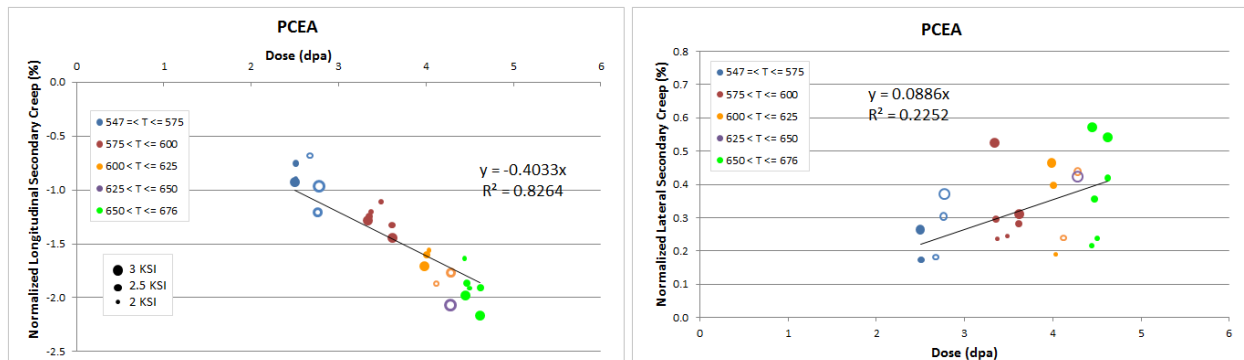

Figure 20. Longitudinal and lateral secondary creep for grade PCEA as calculated from the AGC-2 Creep Rate Calculation Spreadsheet. Results are calculated over the entire AGC-2 temperature (541–681°C) and three stress levels (• = 13.8 MPa, • = 17.2 MPa, • = 20.7 MPa).

Figure 21. Longitudinal and lateral secondary creep for grade IG-110 as calculated from the AGC-2 Creep Rate Calculation Spreadsheet. Results are calculated over the entire AGC-2 temperature (541–681°C) and three stress levels (• = 13.8 MPa, ● = 17.2 MPa, ● = 20.7 MPa).
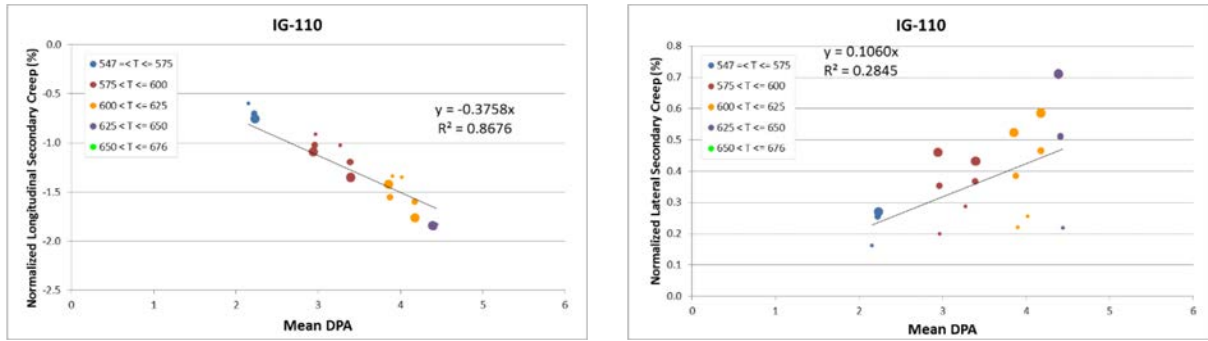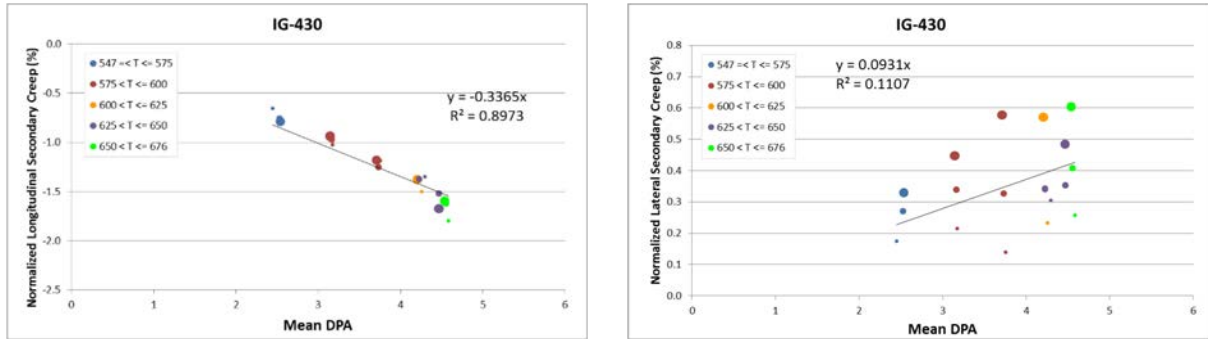

Figure 22. Longitudinal and lateral secondary creep for grade IG-430 as calculated from the AGC-2 Creep Rate Calculation Spreadsheet. Results are calculated over the entire AGC-2 temperature (541–681°C) and three stress levels (• = 13.8 MPa, ● = 17.2 MPa, ● = 20.7 MPa).

All grades exhibit linear creep response and no grade indicates turnaround has been achieved over the temperature and dose ranges of AGC-2 irradiation. The stress-normalized creep shows no particular grouping of similar stress states and all stress levels collapse along a single line, indicating the expected proportional stress dependency. Creep in the axial (longitudinal) direction and creep in the diameter (lateral) direction are markedly different. Dimensional change in the longitudinal direction occurs under compressive stresses, producing a negative strain, while strain in the diametral direction occurs under an induced tensile stress (Poisson's effect), causing a positive strain in the lateral direction. The lateral creep data are somewhat more scattered than the longitudinal changes due, in part, to the specimen sides "barreling" caused by end face friction forces.[4] It should be noted that many of the irradiated specimens did not have a simple "barrel" shape, as the description implies, but formed into a variety of shapes, including hourglass, pear, and out-of-round shapes. This increased the complexity of measuring the diameter changes and subsequently the overall error of those measurements.

PCEA (extruded grade) exhibits the fastest dimensional change, while NBG-18 (vibrationally molded) exhibits the slowest rate. All grades can be seen to exhibit slightly higher creep rates at the higher dose levels and slower rates at the lower dose levels in the less scattered longitudinal directions. This may be attributed to the temperature variations experienced by AGC-2 creep specimens (541–681°C), which are larger than the AGC-2 technical specifications (550–650°C). As illustrated in the AGC-2 thermal analysis,[25,27] specimens located in the central mid-plane region of the irradiation capsule receive the highest flux levels. Consequently, these high flux levels produce the highest heat generation

rates in the capsule, creating higher temperatures within specimens located at the mid-plane. Specimens exposed to similar dose levels but higher temperatures may exhibit a higher rate of dimensional change while specimens exposed to lower temperatures may exhibit lower rates of change. This potential temperature dependence on creep should become clearer with additional analysis after irradiating the AGC-3 and -4 (800°C) and AGC-5 and -6 (1100°C) capsules to establish this dependency.

It is interesting to note that the low-density NBG-17 specimens appear to have an irradiation strain response that is similar to the higher-density specimens. Density is considered to be a major parameter in the irradiation response of nuclear graphite; porosity must be present within the microstructure to accommodate irradiation swelling. Otherwise, turnaround will occur too quickly. Because these low-density specimens are ~15% lower on average, the dimensional change was expected to be lower. However, these results indicate that macroscopic porosity (bulk porosity) has a minimal effect on the irradiation dimensional change behavior of nuclear graphite. The determination of the effect of lower density on irradiation material properties will be described in a future analysis report.

Analysis and comparisons between grades with similar fabrication processes (extruded, isostatically molded, and vibrationally molded) illustrate the creep response due to grain size and raw material differences. Data for the two extruded graphite grades (H-451 and PCEA), the two isostatically molded grades (IG-110 and IG-430), and both vibrationally molded grades (NBG-18 and NBG-17) are shown together in Figure 23, Figure 24, and Figure 25.
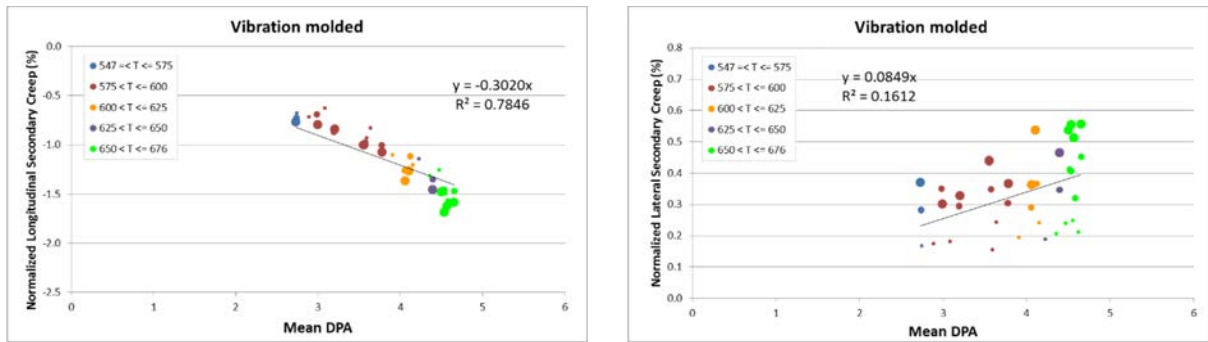

Figure 23. Longitudinal and lateral dimensional change for both vibrationally molded graphite grades (NBG-17 and NBG-18).
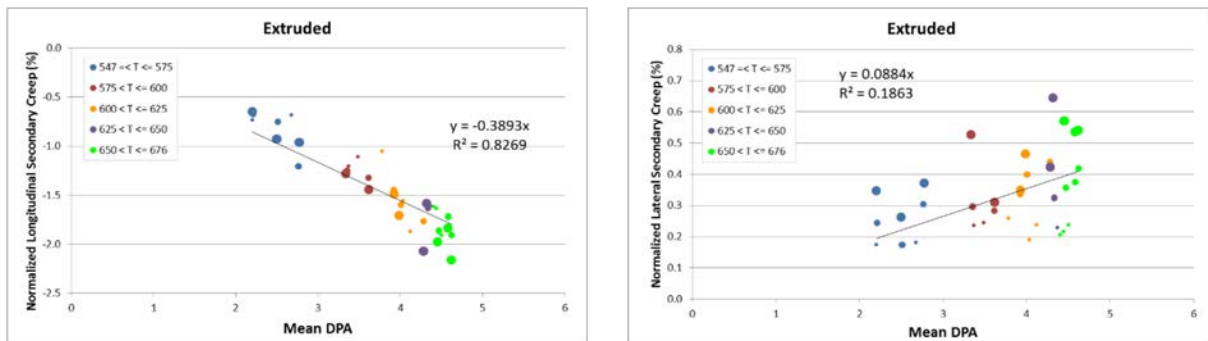

Figure 24. Longitudinal and lateral dimensional change for both extruded graphite grades (H-451 and PCEA).
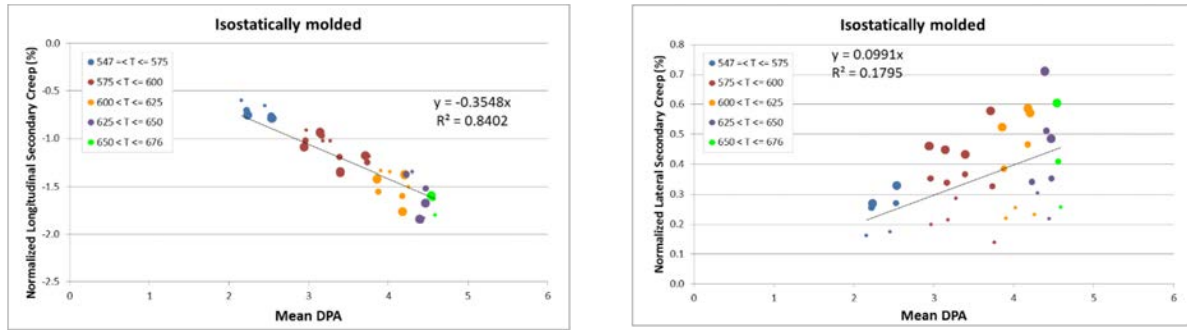
Figure 25. Longitudinal and lateral dimensional change for both isostatically molded graphite grades (IG-110 and IG-430).

As seen, all grades with similar fabrication processes appear to have very similar creep response, with no obvious difference between them. As seen in the AGC-1 analysis, the largest creep strain experienced was for the extruded grades, while the vibrationally and isostatically molded grades experienced generally the same levels of strain. The trend for higher creep rates at high dose levels and lower creep rates for low dose levels noted in the specific grade analysis is more apparent for these data.

9. CREEP AND CREEP COEFFICIENT ANALYSIS BY GRADE

From the AGC-2 Creep Rate Calculation Spreadsheet, the AGC-2 creep coefficients have been calculated for all major graphite grades (Table 8). These creep coefficients are compared to the calculated values for AGC-1 in Figure 26.

It should be noted that the creep coefficient uncertainty is related to the applied stress, dose, and modulus values in addition to the specimen irradiation temperature. Specific uncertainty calculations for AGC-2 have been initiated, with quantitative calculations of the temperature and applied stress levels being determined on a per specimen basis and semi-quantitative estimates of the received dose level.[28] These uncertainty estimates will be applied to the combined "600°C Irradiation" analysis (i.e., AGC-1 and AGC-2 analysis report) to ascertain the total uncertainty over the entire dose range at the nominal 600°C temperature experiments.

Table 8. Calculated longitudinal creep coefficients for AGC-2 and AGC-1 graphite grades irradiated at a nominal 600°C irradiation temperature (K = 10^{-30} cm^2/n·Pa).

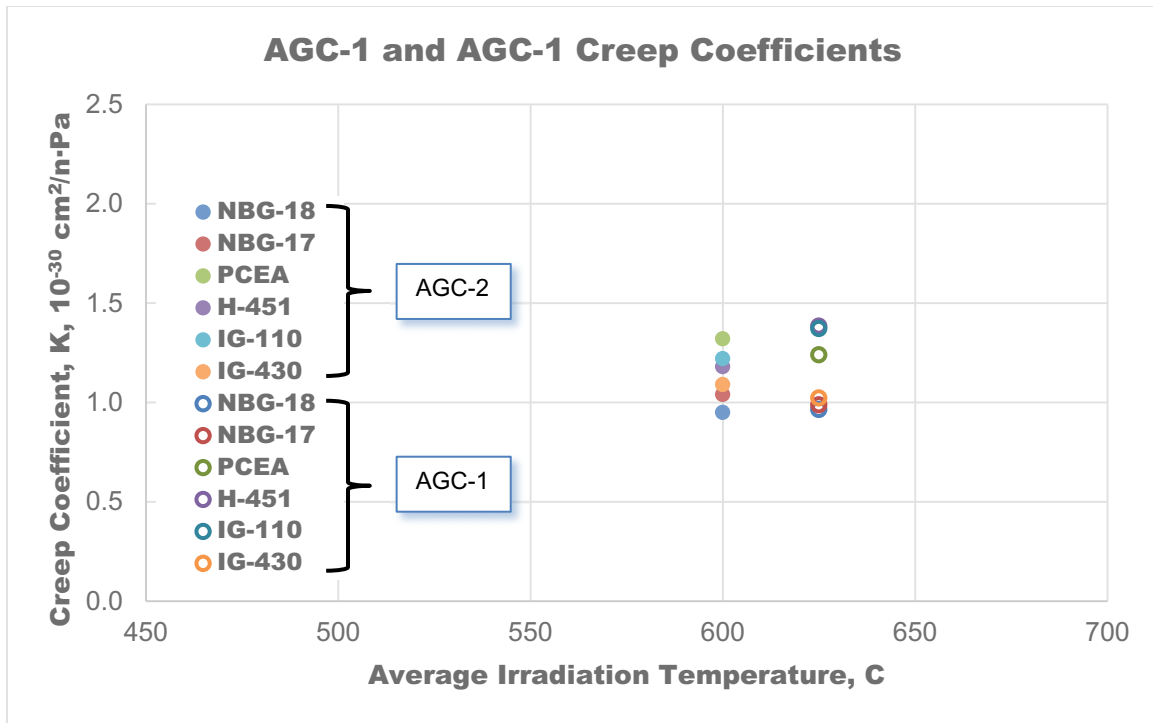| AGC-2			AGC-1		
Average T_{Irr}, °C	K_{Long}	Grade	Average T_{Irr}, °C	K_{Long}	Grade
600	0.095	NBG-18	625	0.096	NBG-18
600	0.104	NBG-17	625	0.099	NBG-17
600	0.132	PCEA	625	0.124	PCEA
600	0.118	H-451	625	0.138	H-451
600	0.122	IG-110	625	0.137	IG-110
600	0.109	IG-430	625	0.102	IG-430

Figure 26. Comparison of AGC-1 and AGC-2 creep coefficients for all major graphite grades.

In general, AGC-2 creep coefficients agree remarkably well with the AGC-1 coefficients even with the large temperature variations between AGC-1 specimens. AGC-2 creep coefficients are compared to previous values calculated from historical creep studies[37,38,39,40,41,42,43,44,45] (Figure 27). This comparison demonstrates the AGC-2 creep coefficients are well within the historical values determined for the irradiation temperatures and dose levels of the AGC-2 test train.
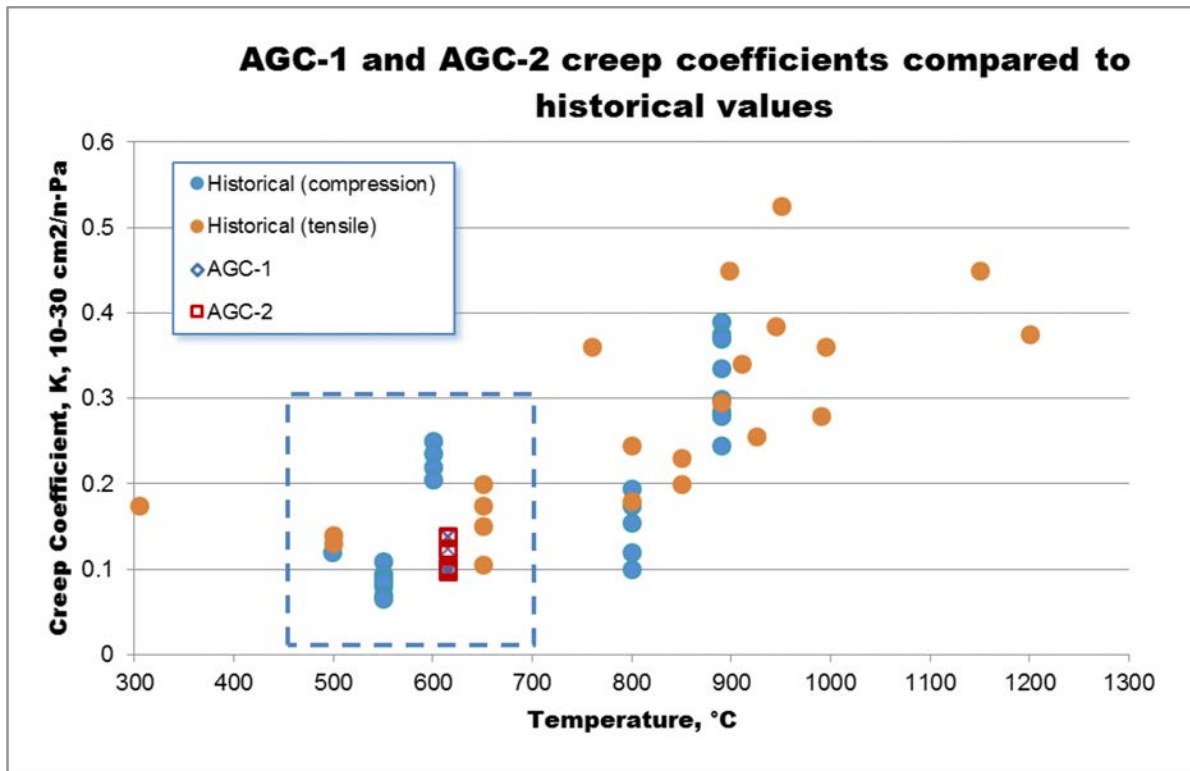
Figure 27. Comparison of AGC-2 creep coefficients to AGC-1 and historical values from previous studies. The dotted lined box illustrates temperature and dose range shown in the previous AGC-1 and AGC-2 creep coefficient values of Figure 26.

AGC-2 and AGC-1 creep coefficients are generally within acceptable and expected levels based on historical creep coefficients at similar irradiation temperatures. Coefficients for all grades are within ~30% of each other, showing remarkable consistency between nuclear grades.

10. CONCLUSIONS

AGC-2 dimensional change, creep strain, and creep coefficients have been analyzed for the six major graphite grades. In general, dimensional change and creep response of AGC-2 major graphite grades were demonstrated to be very similar to those of AGC-1 and prior historical nuclear graphite behavior. Before determining the creep strain and deriving the creep coefficients for the major graphite grades, the dimensional change of the grades was analyzed to ascertain their irradiation behavior. Dimensional behavior for the AGC-2 historical grade (H-451) was found to be similar to previous H-451 measurements, including results from AGC-1. This demonstrates consistency between the AGC experiment and previous irradiation creep studies. The isotropic irradiation behavior for all grades was analyzed by comparing the length and diameter changes for all major grade specimens along with the volumetric behavior of creep (stressed) and control (unstressed) specimens. All grades had isotropic or near-isotropic irradiation response, as demonstrated by the length and diameter dimensional change response.

To assist in the creep strain and complex creep coefficient calculations, a quality assurance QA-validated and -approved spreadsheet was developed to semi-automatically compile and calculate the irradiation-induced creep and creep coefficient for all major graphite grades. The creep response and calculated coefficients for all AGC-2 major grades were reasonable and within expected levels. The AGC-2 creep strain behavior was shown to compare well with previous data from AGC-1 and historical studies.

Specific observations and conclusions from this AGC-2 analysis include the following:

1. Temperature control from AGC-2 creep and control specimens (541–681°C) was much improved over the previous AGC-1 capsule (468–716°C).

2. The larger anisotropic response of the H-451 was expected, however, the larger anisotropic response for IG-430 was surprising.

3. The very high isotropic response from IG-110 was expected; however, the isotropic response for PCEA was very surprising, because it is an extruded grade expected to form a textured microstructure.

4. WG and AG dimensional change was the same for all graphite grades, strongly indicating isotropic irradiation response.

5. While most of the graphite grades demonstrated very similar volumetric response between creep (stressed) and control (unstressed) specimens, there was a measurable difference between the specimens, indicating that volume conservation may not be as strongly predicted as was determined in AGC-1 analysis.

6. The QA-validated semi-automated spreadsheet (i.e., the AGC-2 Creep Rate Calculation Spreadsheet) provided an efficient and accurate method to calculate the creep coefficient as a function of the AGC irradiation variables.

7. Lateral strain measurements have much larger variability. This due to barreling of the cylindrical specimens where Poisson's effect creates lateral tensile stresses with subsequent growth in the specimen diameters. However, the tensile forces are not uniform, and the specimens form into a variety of shapes, including hourglass, pear, and out-of-round shapes. This dramatically increases the complexity of measuring the diameter changes and subsequently increases overall scatter (error) of those measurements.

8. The extruded grades experienced the largest creep strain, while the vibrationally and isostatically molded grades experienced generally the same levels of strain.

9. Calculated AGC-2 creep coefficients for all grades range from 0.095 to 0.132 ($K = 10^{-30}$ cm^2/n·Pa) and are within ~30% of each other, showing remarkable consistency between nuclear grades.

11. REFERENCES

1. T. Burchell, R. Bratton, and W. Windes, *NGNP Graphite Selection and Acquisition Strategy*, ORNL/TM-2007/153, Oak Ridge National Laboratory, September 2007.

2. R. L. Bratton and T. D. Burchell, 2005, *NGNP Graphite Testing and Qualification Specimen Selection Strategy*, INL/EXT-05-00269, Idaho National Laboratory, May 2005.

3. PLN-2497, 2010, "Graphite Technology Development Plan," Rev. 1, Idaho National Laboratory, October 2010.

4. W. E. Windes, W. D. Swank, D. T. Rohrbaugh, and D. L. Cottle, *AGC-2 Specimen Post-Irradiation Data Package Report*, INL/EXT-15-36244, Idaho National Laboratory, August 2015.

5. TFR-645, 2010, "Advanced Graphite Capsule AGC-2 Experiment Test Train," Rev. 0, Idaho National Laboratory, July 2010.

6. T. Burchell and R. Bratton, 2005, *Graphite Irradiation Creep Capsule AGC-1 Experimental Plan*, ORNL/TM-2005/505, Oak Ridge National Laboratory, May 2005.

7. INL Drawing 600786, 2009, "ATR Advanced Graphite Capsule (AGC-2) Graphite Specimen Machining Details," Rev. 1, Idaho National Laboratory, March 2009.

8. INL Drawing 600786, 2012, "ATR Advanced Graphite Capsule (AGC-2) Graphite Specimen Machining Details," Rev. 2, Idaho National Laboratory, July 2012.

9. INL Drawing 600787, 2010, "ATR Advanced Graphite Capsule (AGC-2) Experiment Graphite Specimen Cut-Out Diagrams," Rev. 3, Idaho National Laboratory, July 2010.

10. INL Drawing 601266, 2012, "ATR Advanced Graphite Capsule Number 2 (AGC-2) Capsule Facility Assemblies," Rev. 2, Idaho National Laboratory, July 2012.

11. INL Drawing 601258, 2012, "ATR Advanced Graphite Capsule 2 (AGC-2) Graphite Specimen Holder Assemblies and Details," Rev. 1, Idaho National Laboratory, July 2012.

12. INL Drawing 600001, 2009, "ATR TMIST-1 Oxidation Experiment In-Vessel Installation," Rev. 2, Idaho National Laboratory, March 2009.

13. J. R. Parry, 2010, "Engineering Calculations and Analysis Report: Reactor Physics Projections for the AGC-2 Experiment Irradiated in the ATR South Flux Trap," ECAR-1050, Rev. 0, Idaho National Laboratory, October 13, 2010.

14. T. Burchell, 2009, *A Revised AGC-1 Creep Capsule Layout*, ORNL/TM-2009/009, Oak Ridge National Laboratory, January 2009.

15. T. Burchell, J. Strizak, and M. Williams, 2011, *AGC-1 Specimen Preirradiation Data Report*, ORNL/TM-2010/285, Oak Ridge National Laboratory, August 2011.

16. T. Reed, 2012, "AGC-1 Individual Fluence, Temperature, and Load Calculation and Tabulation," ECAR-1943, Idaho National Laboratory, September 2012.

17. T. Reed, 2012, "AGC-1 As Run Thermal Results," ECAR-1944, Idaho National Laboratory, September 2012.

18. L. Hull, 2012, *AGC-2 Irradiation Data Qualification Final Report*, INL/EXT-12-26248, Idaho National Laboratory, July 2012.

19. TFR-645, 2010, "Advanced Graphite Capsule AGC-2 Experiment Test Train," Rev. 0, Idaho National Laboratory, July 2010.

20. D. Swank, 2010, *AGC-2 Graphite Preirradiation Data Package*, INL/EXT-10-19588, Rev. 0, Idaho National Laboratory, August 2010.

21. R. G. Ambrosek, "Thermal Projections for AGC-2," ECAR-1161, Idaho National Laboratory.

22. M. Davenport, 2010, "Engineering Work Instructions for Assembling the AGC-2 Experiment," Quality Assurance Record: QA# 137268, Idaho National Laboratory, October 2010.

23. W. Windes, 2014, *AGC-2 Disassembly Report*, INL/EXT-14-32060, Idaho National Laboratory, May 2014.

24. D. Swank, AGC-2 Graphite Specimen Postirradiation Characterization Plan," PLN-4657, Rev. 0, Idaho National Laboratory.

25. J. R. Parry, "As-Run Physics Analysis for the AGC-2 Experiment Irradiated in the ATR", Idaho National Laboratory, ECAR-2291, March 2014.

26. Rohrbaugh, David, "AGC-2 Specimen Load Calculations by Stack," ECAR-2925, Idaho National Laboratory, February 2016.

27. P. E. Murray, "As·Run Thermal Analysis of the AGC-2 Experiment," ECAR-2322, Idaho National Laboratory, April 2014.

28. D. T. Rohrbaugh, W. D. Swank, W. E. Windes, *AGC-2 Irradiation Report*, INL/EXT-16-38431, Idaho National Laboratory, June 2016.

29. T. D. Burchell, *AGC-1 Irradiation Creep Strain Data Analysis*, ORNL/TM-2014/255, Oak Ridge National Laboratory, September 2014.

30. T. D. Burchell, *AGC-1 Irradiation Induced Property Changes Analysis Report: Electrical Resistivity and Coefficient of Thermal Expansion*, ORNL/TM-2015/377, Oak Ridge National Laboratory, February 2016.

31. P. E. Murray, "Uncertainty Analysis of Temperature in the AGC-1 and AGC-2 Experiments," ECAR-3017, Idaho National Laboratory, April 2016.

32. B. T. Kelly and J. E. Brocklehurst, "UKAEA reactor group studies of irradiation induced creep in graphite," *Journal of Nuclear Materials*, Vol. 65, No. 1, 1977, pp. 79–85.

33. B. T. Kelly and A. J. E. Foreman, "Theory of irradiation creep in reactor graphite—dislocation pinning-unpinning model," Carbon, Vol. 12, No. 2, 1974, pp. 151–158.

34. B. T. Kelly and T. D. Burchell, "The Analysis of Irradiation Creep Experiments on Nuclear Reactor Graphite," Carbon, Vol. 32, No. 1, 1994, pp. 119–125.

35. T. D. Burchell, *Irradiation Induced Creep in Graphite at High Temperature and Dose – A Revised Model*, ORNL/TM-2008/098, Oak Ridge National Laboratory, February 2009.

36. W. D. Swank, "Form 562.41 - AGC-2 Creep Rate Calculation Spreadsheet," Idaho National Laboratory Electronic Data Management System (EDMS), July 2016.

37. W. J. Gray, "Constant stress irradiation-induced compressive creep of graphite at high fluences", Carbon, Vol. 11, 1973, pp. 383–392.

38. C. R. Kennedy, W. H. Cook and W. P. Eatherly, "Results of Irradiation Creep Testing Graphite at 900°C", American Carbon Conference, 13th Biennial Conference., Irvine, California, 1977, pp.342-343.

39. M. A. Cundy and G. Kleist, "Irradiation Creep to Very High Neutron Fluences,", CARBONE 84: International Carbon Conference on Carbon and Graphite, in Transactions Carbone 84, Bordeaux, France, July 1984, pp 406-407.

40. T. Oku, M. Eto and S. Ishiyama, "Irradiation Creep Properties and Strength of a Fine-Grained Isotropic Graphite", JNM, 172 (1990) pp. 77-84.

41. R.Blackstone, L.W. Graham, and M.R. Everett, "High Temperature Radiation Induced Creep in Graphite", American Carbon Society, 9th Biennial Conference, Boston, MA, 1969.

42. H. J. Veringa and R. Blackstone, "The Irradiation Creep in Reactor Graphites for HTR Applications", Carbon, 1976. Vol. 14, pp. 279-285.

43. B. T. Kelly, "Irradiation Creep in Graphite - Some New Considerations and Observations", Carbon Vol. 30. No. 3, pp. 379-383. 1992

44. C, R. Kennedy, M. Cundy, G. Kleist, "The Irradiation Creep Characteristics of Graphite to High Fluences", Proceedings of CARBONE 88: International Carbon Conference on Carbon and Graphite, in Transactions Carbone 88, Newcastle, UK, 1988, pp. 443-445.

45. Ph.D Thesis. A. S. Mobasheran, University of Tennessee, Dec. 1990.